A search for the dimuon decay of the Standard Model Higgs boson with the ATLAS detector

The ATLAS Collaboration

A search for the dimuon decay of the Standard Model (SM) Higgs boson is performed using data corresponding to an integrated luminosity of $139\,\text{fb}^{-1}$ collected with the ATLAS detector in Run 2 pp collisions at $\sqrt{s} = 13$ TeV at the Large Hadron Collider. The observed (expected) significance over the background-only hypothesis for a Higgs boson with a mass of 125.09 GeV is 2.0σ (1.7σ). The observed upper limit on the cross section times branching ratio for $pp \to H \to \mu\mu$ is 2.2 times the SM prediction at 95% confidence level, while the expected limit on a $H \to \mu\mu$ signal assuming the absence (presence) of a SM signal is 1.1 (2.0). The best-fit value of the signal strength parameter, defined as the ratio of the observed signal yield to the one expected in the SM, is $\mu = 1.2 \pm 0.6$.

Contents

1 Introduction

In July 2012, the ATLAS and CMS Collaborations announced the discovery of a new particle with a mass of approximately 125 GeV [1, 2] at the CERN Large Hadron Collider (LHC). Subsequent measurements have indicated that this particle is consistent with the Standard Model (SM) Higgs boson [3–6], denoted by H. While the interaction between the Higgs boson and the charged fermions of the third-generation has already been observed by both the ATLAS and CMS Collaborations [6–10], only upper limits have been set on the interactions with fermions of the other generations. The $H \rightarrow \mu\mu$ decay offers the best opportunity to measure the Higgs interactions with a second-generation fermion at the LHC. The SM branching ratio to dimuons for the Higgs boson with $m_H = 125.09$ GeV is $(2.17 \pm 0.04) \times 10^{-4}$ [11]. However, physics beyond the SM [12, 13] could modify the branching ratio.

Both the ATLAS and CMS Collaborations carried out searches for the $H \rightarrow \mu\mu$ process based on partial sets of about one quarter of the data collected during Run 2 of the LHC [14, 15]. This paper presents an improved search for the dimuon decay of the Higgs boson using the full pp collision dataset recorded with the ATLAS detector in the LHC Run 2 period, spanning 2015 to 2018 at $\sqrt{s} = 13$ TeV, corresponding to an integrated luminosity of about 139 fb^{-1}. Compared to the previous publication [14], several improvements have been made. They include a better categorisation based on multivariate techniques that exploit the topological and kinematic differences between the different signal production modes and the background processes, improvements in the muon reconstruction, a large increase in the equivalent integrated luminosity

of the simulated background samples using a dedicated fast simulation, and an improved methodology for the background modelling.

The analysis selects events with two opposite-charge muons and classifies them into 20 mutually exclusive categories based on the event topology and multivariate discriminants to increase the signal sensitivity. After event categorisation, the signal yield is extracted by a simultaneous fit to the 20 dimuon mass ($m_{\mu\mu}$) distributions in the range 110–160 GeV together with background normalisation and shape parameters, exploiting the resonant behaviour of the Higgs boson signal. The Higgs boson is assumed to have a mass of m_H = 125.09 GeV [5] for all results presented. More recent measurements of the Higgs boson mass [16, 17] are compatible within their uncertainties with this value.

2 ATLAS detector

The ATLAS detector [18, 19] covers nearly the entire solid angle around the collision point.[1] It consists of an inner tracking detector surrounded by a thin superconducting solenoid, electromagnetic and hadronic calorimeters, and a muon spectrometer incorporating three large superconducting toroid magnets.

The inner detector (ID) system is immersed in a 2 T axial magnetic field and provides charged-particle tracking in the range $|\eta| < 2.5$. A high-granularity silicon pixel detector covers the vertex region and typically provides four measurements per track. It is surrounded by a silicon microstrip tracker, which typically provides four measurement points per track. These silicon detectors are complemented by a transition radiation tracker, which enables radially extended track reconstruction up to $|\eta| = 2.0$.

The calorimeter system covers the pseudorapidity range $|\eta| < 4.9$. Within the region $|\eta| < 3.2$, electromagnetic calorimetry is provided by barrel and endcap high-granularity liquid-argon (LAr) sampling calorimeters, with an additional thin LAr presampler covering $|\eta| < 1.8$ to correct for energy loss in material upstream of the calorimeters. Hadronic calorimetry is provided by a scintillator-tile calorimeter, segmented into three barrel structures within $|\eta| < 1.7$, and two LAr hadronic endcap calorimeters.

The muon spectrometer (MS) comprises separate trigger and high-precision tracking chambers measuring the deflection of muons in a magnetic field generated by the superconducting air-core toroids. The precision chamber system covers the region $|\eta| < 2.7$ with three layers of monitored drift tubes, complemented by cathode-strip chambers in the forward region, where the background is highest. The muon trigger system covers the range $|\eta| < 2.4$ with resistive-plate chambers in the barrel, and thin-gap chambers in the endcap regions.

The data were collected with a two-level trigger system [20]. The first-level trigger (L1) is implemented in hardware and uses a subset of the detector information. This is followed by a software-based high-level trigger which runs algorithms similar to those in the offline reconstruction software, reducing the event rate to approximately 1 kHz from the maximum L1 rate of 100 kHz.

---

[1] ATLAS uses a right-handed coordinate system with its origin at the nominal interaction point (IP) in the centre of the detector and the z-axis along the beam pipe. The x-axis points from the IP to the centre of the LHC ring, and the y-axis points upward. Cylindrical coordinates (r, ϕ) are used in the transverse plane, ϕ being the azimuthal angle around the z-axis. The pseudorapidity is defined in terms of the polar angle θ as $\eta = -\ln\tan(\theta/2)$. The rapidity is defined as $y = \frac{1}{2}\ln\frac{E+p_z}{E-p_z}$ and the distance between two objects is defined as $\Delta R = \sqrt{(\Delta y)^2 + (\Delta\phi)^2}$.

3 Data and simulated event samples

The pp collision data at $\sqrt{s} = 13$ TeV analysed here correspond to the full recorded Run 2 dataset, with an integrated luminosity of $139\,\text{fb}^{-1}$ after the application of data quality requirements. The mean number of pp interactions per bunch crossing was about 34. Events used in this analysis were recorded using a combination of single-muon triggers with transverse momentum thresholds up to 26 GeV for isolated muons and 50 GeV for muons without any isolation requirement imposed, allowing to recover some inefficiency introduced by the isolation requirement at trigger level for high momentum muons. The trigger efficiency for the sum of the $H \rightarrow \mu\mu$ signal processes is about 91% relative to the common event preselection discussed in Section 4.

Samples of simulated Monte Carlo (MC) events are used to optimise the selection, to model the signal processes and to develop an analytic function to model the $m_{\mu\mu}$ distributions for the background estimate. The signal samples as well as a complete set of background processes were processed through the full ATLAS detector simulation [21] based on Geant4 [22], henceforth referred to as fully simulated samples.

Signal samples were generated for the main Higgs boson production modes. The mass of the Higgs boson was set in the simulation to $m_H = 125$ GeV and the corresponding width is $\Gamma_H = 4.07$ MeV [23]. The samples are normalised with the latest available theoretical calculations of the corresponding SM production cross sections, summarised in Ref. [11]. The normalisation of all Higgs boson samples also accounts for the $H \rightarrow \mu\mu$ branching ratio of 2.17×10^{-4} calculated with HDECAY [24–27] and PROPHECY4F [28–30].

Higgs boson production in the gluon–gluon fusion process (ggF) was simulated using the Powheg NNLOPS program [31–38] with the PDF4LHC15 set of parton distribution functions (PDFs) [39]. The simulation achieves next-to-next-to-leading-order (NNLO) accuracy in QCD for inclusive observables after reweighting the Higgs boson rapidity spectrum [40]. The parton-level events were processed by Pythia 8 [41] to decay the Higgs bosons and to provide parton showering, final-state photon radiation (QED FSR), hadronisation and the underlying event, using the AZNLO set of tuned parameters [42]. The sample is normalised to a next-to-next-to-next-to-leading-order QCD calculation with next-to-leading-order (NLO) electroweak corrections [43–54].

Higgs bosons produced via vector-boson fusion (VBF) and in association with a vector boson, $q\bar{q}/qg \rightarrow VH$ with $V = W$ or Z, were generated at NLO accuracy in QCD using the Powheg-Box program [55–57]. The loop-induced process $gg \rightarrow ZH$ was generated at leading order (LO) using Powheg-Box. For the VBF and VH samples the same settings for the PDF set and Pythia 8 as in the ggF sample were employed. The VBF sample is normalised to an approximate-NNLO QCD cross section with NLO electroweak corrections [58–60]. The VH samples are normalised to cross sections calculated at NNLO in QCD with NLO electroweak corrections for $q\bar{q}/qg \rightarrow VH$ and at NLO and next-to-leading-logarithm accuracy in QCD for $gg \rightarrow ZH$ [61–68]. Higgs boson production in association with a top-quark pair, $t\bar{t}H$, was simulated at NLO accuracy in QCD using MadGraph5_aMC@NLO [69, 70] with the NNPDF3.0NLO PDF set [71] and interfaced to Pythia 8 using the A14 set of tuned parameters [72]. The cross section is taken from a calculation accurate to NLO in QCD with NLO electroweak corrections [73–76].

Background events from the Drell–Yan (DY) $Z/\gamma^* \rightarrow \mu\mu$ process were generated with Sherpa 2.2.1 [77] using NLO-accurate matrix elements for up to two partons, and LO-accurate matrix elements for up to four partons calculated with the Comix [78] and OpenLoops [79, 80] libraries and the NNPDF3.0 NNLO set. They were matched to the Sherpa parton shower [81] using the MEPS@NLO prescription [82–85]. Diboson processes (WW, WZ, and ZZ) as well as electroweak Zjj production were simulated in a similar set-up with Sherpa 2.2.1. The $t\bar{t}$ and single-top-quark samples were generated at NLO accuracy with

Powheg-Box [86, 87] using the NNPDF3.0NLO PDF set interfaced to Pythia 8 for parton showering and hadronisation using the A14 parameter set. For the Wt process, the diagram removal scheme [88] is applied to remove the overlap with $t\bar{t}$ production. The production of $t\bar{t}V$ events was modelled using the MadGraph5_aMC@NLO [69] generator at NLO in a set-up similar to the one used for the $t\bar{t}H$ process.

The effects of multiple pp collisions in the same or neighbouring bunch crossings (pile-up) are included in the MC simulation by overlaying inelastic pp interactions produced using Pythia 8 with the NNPDF2.3LO set of PDFs [89] and the A3 set of tuned parameters [90]. Events are reweighted such that the distribution of the average number of interactions per bunch crossing matches that observed in data. Simulated events are corrected to reflect the momentum scales and resolutions as well as the trigger, reconstruction, identification, and isolation efficiencies measured in data for all the physics objects used in this analysis.

The background samples discussed above provide an equivalent integrated luminosity that is typically 5–20 times higher than that of data and are used to train multivariate classifiers and to test the background modelling. However, the statistical uncertainties in the dominant DY background are a limiting factor in studying the background modelling at the level required by the small expected $H \to \mu\mu$ signal. Therefore, two fast-simulation set-ups were developed to generate significantly larger DY samples. The primary fast-simulation DY sample is based on parton-level events generated [91] with Sherpa 2.2.4 [92] using LO matrix elements for Z/γ^* production with up to three additional partons and using the CT14 NNLO PDF set [93]. The parton-level events were processed with Pythia 8 to provide QED and QCD parton showering and hadronisation, and double-counted QCD emissions were removed using the CKKW-L algorithm [94] with a merging scale of 20 GeV. For further cross-checks, an additional fast-simulation DY sample was prepared that simulates $Z/\gamma^* + 0, 1$ partons inclusively at NLO accuracy using Powheg-Box [95] with the CT10 PDF set [96] and $Z/\gamma^* + 2$ partons at LO accuracy with Alpgen [97] using the CTEQ6L1 PDF set [98]. These parton-level events were processed with an approximate QCD shower algorithm, overlaps between the two samples were removed, and QED FSR was provided by Photos [99]. For both of these generated samples, experimental effects were approximated using parameterisations rather than using the full ATLAS detector simulation and reconstruction software. The parameterisations, extracted from fully simulated MC samples or directly from ATLAS data, reproduce the reconstruction and selection efficiencies of detector-level objects by event weighting and model the resolution of the ATLAS detector with predetermined probability distributions. Detailed descriptions were employed for the muon momentum resolution and muon trigger and selection efficiencies, for the photons from QED FSR, for hadronic jets from the primary interaction and pile-up events in terms of kinematics and the number of associated ID tracks, and for the effect of pile-up and the underlying event on the measurement of the missing transverse momentum $E_{\text{T}}^{\text{miss}}$. In total, two sets of about 10–20 billion events are prepared in this way, corresponding to an equivalent integrated luminosity of at least $50 \, \text{ab}^{-1}$ in the kinematic phase space relevant for the analysis.

Both fast simulation DY samples give a good description of the data distributions of the observables used in this analysis to discriminate the DY background from the $H \to \mu\mu$ signal, i.e. the $m_{\mu\mu}$ mass spectra and the multivariate discriminants described in the following sections. Small residual differences are taken into account by reweighting the mass spectra to the data sidebands as described in Section 6.

4 Object definitions and event selection

Events are required to contain at least one reconstructed pp collision vertex candidate with at least two associated ID tracks each with $p_{\text{T}} > 0.5 \, \text{GeV}$. The vertex with the largest sum of p_{T}^2 of tracks is considered

to be the primary vertex of the hard interaction. For signal events the primary vertex selection criteria has an efficiency of about 99% [100].

The majority of muon candidates are reconstructed by combining a track in the ID with a track in the MS. To improve the muon reconstruction efficiency in the region of $|\eta| < 0.1$, which has limited coverage in the MS, additional muon candidates are identified by matching a reconstructed ID track to either an MS track segment or a calorimetric energy deposit consistent with a minimum-ionising particle. In the region $2.5 < |\eta| < 2.7$, which is not covered by the ID, additional muons are reconstructed from an MS track with hits in the three MS layers and combined with forward ID hits, if possible. Muon candidates are required to satisfy the 'loose' criteria defined in Ref. [100] and have $p_T > 6\,\text{GeV}$ and $|\eta| < 2.7$. Muons with an associated ID track must be matched to the primary vertex by having a longitudinal impact parameter z_0 that satisfies $|z_0 \sin(\theta)| < 0.5$ mm, where θ is the polar angle of the track. The significance of the transverse impact parameter d_0 calculated relative to the measured beam-line position is required to be $|d_0|/\sigma(d_0) < 3$, where $\sigma(d_0)$ is the uncertainty in d_0. Furthermore, isolation criteria are applied to suppress non-prompt muons originating from hadron decays. The isolation selection uses information about ID tracks and calorimeter energy deposits in a range $\Delta R < 0.2$ around the muon as described in Ref. [101].

Since muons may lose a significant fraction of their energy by QED FSR, up to one final-state photon candidate per event is included in the $m_{\mu\mu}$ calculation to improve the signal reconstruction. Photon candidates are reconstructed with a procedure similar to the one described in Ref. [101], optimised to achieve the best sensitivity for the $H \to \mu\mu$ signal. Only photon candidates close to muons ($\Delta R(\gamma, \mu) < 0.2$) are considered. To reduce background from pile-up interactions, a variable threshold is imposed on the photon transverse momentum p_T^γ; the threshold increases linearly from $p_T^\gamma = 3\,\text{GeV}$ for $\Delta R = 0$ to $p_T^\gamma = 8\,\text{GeV}$ for $\Delta R = 0.2$. If more than one photon passes this requirement, the photon with the highest transverse momentum is selected. A QED FSR candidate is found in about 5% of the events and the signal $m_{\mu\mu}$ width is reduced by about 3% when considering all reconstructed signal events. With these selections, contributions from the loop-induced decay $H \to Z\gamma, Z \to \mu\mu$ [102] are expected to be around 0.1% of the $H \to \mu\mu$ yield and are thus neglected in the further analysis.

Electrons are reconstructed by matching clusters of energy in the electromagnetic calorimeter to tracks in the ID. They are required to satisfy 'Medium' identification criteria [103], have $p_T > 7\,\text{GeV}$ and $|\eta| < 2.47$ and be outside the region of $1.37 < |\eta| < 1.52$. Similarly to muons, electrons are required to be isolated from additional activity measured by ID tracks and the calorimeters within $\Delta R < 0.2$ [101] and to be matched to the primary vertex with $|z_0 \sin(\theta)| < 0.5$ mm and $|d_0|/\sigma(d_0) < 5$.

Jets are reconstructed from 'particle flow' objects [104] using the anti-k_t algorithm [105, 106] with a radius parameter of $R = 0.4$. Candidate jets must have $|\eta| < 4.5$, and the jet p_T must be larger than 25 (30) GeV for $|\eta| < 2.4$ ($2.4 < |\eta| < 4.5$). To suppress pile-up contributions, jets with $|\eta| < 2.4$ and $p_T < 60\,\text{GeV}$ that do not originate from the primary vertex are rejected using the jet vertex tagging algorithm (JVT) [107], which combines tracking information into a multivariate likelihood.

Jets containing b-hadrons with $|\eta| < 2.5$ are identified as b-tagged jets using a multivariate b-tagging algorithm. Two identification working points (WP) are used [108, 109] to provide a 60% (85%) efficiency in $t\bar{t}$ events and a rejection factor of 1200 (25) for light-flavour jets, respectively.

Neutrinos escape from the detector and lead to missing transverse momentum E_T^{miss}. The E_T^{miss} is defined as the magnitude of the negative vectorial sum of the transverse momenta of the selected and calibrated physics objects (including muons, electrons and jets) and the ID tracks not associated with any physics object (soft term) [110, 111].

Table 1: Summary of the main event selection criteria common to all events as well as the criteria applied to the selection of hadronic jets. The bottom sections give the basic requirements on leptons and b-tagged jets for the analysis categories targeting different Higgs boson production processes. The subleading muon momentum threshold is 15 GeV in all categories except the VH 3-lepton categories, where it is lowered to 10 GeV.

	Selection
Common preselection	Primary vertex Two opposite-charge muons Muons: $|\eta| < 2.7$, $p_T^{lead} > 27$ GeV, $p_T^{sublead} > 15$ GeV (except VH 3-lepton)
Fit Region	$110 < m_{\mu\mu} < 160$ GeV
Jets	$p_T > 25$ GeV and $|\eta| < 2.4$ or with $p_T > 30$ GeV and $2.4 < |\eta| < 4.5$
$t\bar{t}H$ Category VH 3-lepton Categories VH 4-lepton Category ggF +VBF Categories	at least one additional e or μ with $p_T > 15$ GeV, at least one b-jet (85% WP) $p_T^{sublead} > 10$ GeV, one additional e (μ) with $p_T > 15(10)$ GeV, no b-jets (85% WP) at least two additional e or μ with $p_T > 8, 6$ GeV, no b-jets (85% WP) no additional μ, no b-jets (60% WP)

Events are selected if they contain at least two opposite-charge muon candidates. The leading muon is required to have $p_T > 27$ GeV to be above the trigger threshold and in most categories the subleading muon has to have $p_T > 15$ GeV. Further requirements on the presence or absence of additional muons, electrons and b-tagged jets depend on the targeted Higgs boson production mode ($t\bar{t}H$, VH, or ggF +VBF), as detailed in Section 5. The main selection requirements are summarised in Table 1. The final signal+background fits are performed in the region $m_{\mu\mu} = 110–160$ GeV, where about 450 000 data events are selected. Within the mass window $m_{\mu\mu} = 120–130$ GeV, which contains about 85% of the signal, about 868 $H \rightarrow \mu\mu$ events are expected. This corresponds to a total efficiency times acceptance of about 52% with respect to all $H \rightarrow \mu\mu$ produced in the ggF, VBF, VH and $t\bar{t}H$ processes.

5 Event categorisation

Events satisfying the preselection criteria of Section 4 are classified into 20 mutually exclusive categories. They are defined to exploit the topological and kinematic differences between the background processes and the different Higgs boson production modes: ggF, VBF, VH and $t\bar{t}H$. The background is dominated inclusively by the DY process, while diboson production, $t\bar{t}$ and single-top production and rarer SM processes such as $t\bar{t}V$ play a significant role in the categories targeting VH and $t\bar{t}H$ production.

After preselecting events according to the presence of additional leptons and the number of jets and b-tagged jets, boosted decision trees (BDT) [112, 113] are trained using the XGBoost package [114] to enhance the signal sensitivity as explained in the following. In order to avoid any potential bias, all trainings are performed using k-fold cross-validation, where k different partitions are used in turn for training, for validation and for testing.

The category selections targeting the different Higgs boson production modes are made in a specific exclusive order, corresponding to the order in which they are presented in this section.

5.1 $t\bar{t}H$ category

A category enriched in $t\bar{t}H$ events is defined in order to target the dileptonic or semileptonic decay of the $t\bar{t}$ system. Events are considered for this category if there is at least one lepton (e or μ) with a transverse momentum $p_T > 15$ GeV in addition to the opposite-sign muon pair and at least one b-tagged jet selected by the 85% efficiency working point. The two highest-p_T muons with opposite charge are chosen as the Higgs boson decay candidate and used to calculate the variable $m_{\mu\mu}$ used in the final fit. This procedure correctly selects the muon pair coming from the Higgs boson decay in about 80% of the cases. After this selection, a BDT is trained using simulated $t\bar{t}H$, $H \rightarrow \mu\mu$ events as signal and simulated events from all SM background processes as background, both selected in a range $m_{\mu\mu} = 100$–200 GeV. The 12 variables used in the BDT include the Higgs boson candidate's transverse momentum $p_T^{\mu\mu}$, the value of the cosine of the lepton decay angle $\cos\theta^*$ in the Collins–Soper frame [115], the transverse momenta of the additional leptons, the multiplicity of central jets with $|\eta| < 2.5$, the multiplicity of b-tagged jets, and the scalar sum of the transverse momenta of all the jets, H_T. In addition, several invariant masses derived from the reconstructed objects as described in the following are used. If there are not enough reconstructed objects in the event to define the invariant masses described in the following, fixed arbitrary values outside their physical ranges are assigned. The leptonic top-quark candidate mass $m_{\text{Lep-Top}}$ is calculated as the transverse mass of the system composed of the third lepton, the missing transverse momentum and the b-tagged jet candidate (if more than one b-tagged jet is present, the one yielding $m_{\text{Lep-Top}}$ closest to 173 GeV is chosen). The transverse mass of the leptonic W-boson candidate $m_{\text{Lep-}W}$ is calculated from the system composed of the third lepton and the missing transverse momentum. The hadronic top-quark candidate mass $m_{\text{Had-Top}}$ is reconstructed from three jets, where one jet must be b-tagged (if only one b-tagged jet is present, it is used in the reconstruction of both $m_{\text{Lep-Top}}$ and $m_{\text{Had-Top}}$). If more than three jets are available, the combination is chosen that maximises the probability of compatibility with a hadronic top-quark decay in terms of closeness of $m_{\text{Had-Top}}$ and $m_{\text{Had-}W}$ to the top-quark and W-boson masses, respectively, where the mass of the hadronically decaying W boson, $m_{\text{Had-}W}$, is calculated from the two non-b-tagged jets associated with the hadronic top decay. If, in addition to the two muons associated with the Higgs boson candidate, two additional opposite-sign and same-flavour leptons are present in the event, their invariant mass is used in the BDT. Similarly, if there are at least three muons reconstructed, the mass of the dimuon pair formed from the muon with the third-highest p_T and the oppositely charged muon assigned to the Higgs boson is included in the classification.

A selection is applied to the BDT score to define one $t\bar{t}H$-enriched category (named $t\bar{t}H$ in the following) by optimising the sensitivity to the predicted SM signal. The background is expected to be dominated by the $t\bar{t}Z$ process with additional contributions from the production of $t\bar{t}$, dibosons, and $t\bar{t}H$ with Higgs boson decays into a final state different from $H \rightarrow \mu\mu$. Assuming SM Higgs boson production and decay, 1.2 signal events are expected in this category with a purity of 98% for the $t\bar{t}H$ process relative to other Higgs boson production modes and a signal-to-background ratio of 8% in the mass window $m_{\mu\mu} = 120$–130 GeV.

5.2 VH categories

Events not selected in the $t\bar{t}H$ category are considered for the VH-enriched categories. The VH categories target signal events where the Higgs boson is produced in association with a leptonically decaying vector boson, $W \rightarrow \ell\nu$ or $Z \rightarrow \ell\ell$ with $\ell = e, \mu$, drastically reducing the DY background. Events are required to have no jets identified as b-jet candidates by the b-tagging algorithm at the 85% efficiency working

point. In addition to a pair of oppositely charged muons from the $H \to \mu\mu$ decay, at least one additional isolated muon or electron must be reconstructed. In events with exactly three leptons, the subleading muon associated with the Higgs boson candidate is required to have a transverse momentum of at least 10 GeV, the additional muon (electron) is required to have a transverse momentum of at least 10 (15) GeV and no $Z \to \mu\mu$ candidate, defined as an opposite-charge dimuon pair with a mass $m_{\mu\mu} = 80$–105 GeV, can be present. In events with at least four leptons, the two additional leptons (muons or electrons) are required to have transverse momenta of at least 8 and 6 GeV and at most one $Z \to \mu\mu$ candidate can be present. If more than two muons are reconstructed, their assignment to the $H \to \mu\mu$ and $Z \to \mu\mu$ ($W \to \mu\nu$) decay candidates is based on their charges and on the minimisation of a χ^2 criterion that takes into account the difference between the reconstructed and expected (transverse) masses of the two bosons and their expected experimental resolutions. In the three-lepton case, the χ^2 makes use of the transverse mass built from the lepton associated with the W boson, called the 'W lepton' henceforth, and the missing transverse momentum. For these topologies the correct pairing is obtained in 93% and 97% of the cases for the four-lepton and three-lepton channels, respectively. If the additional leptons are electrons, these are matched without ambiguity to the $W \to e\nu$ or $Z \to ee$ decays. The two muons chosen as the $H \to \mu\mu$ candidate are used to calculate the variable $m_{\mu\mu}$ used in the final fit.

Two BDTs are trained, separately for the three-lepton and four-lepton events, to discriminate between the simulated signal and background events satisfying the preselection criteria and having a dimuon invariant mass in the range $m_{\mu\mu} = 110$–160 GeV. The three-lepton BDT uses the WH, $H \to \mu\mu$ production as signal. The variables used include the azimuthal separation $\Delta\phi$ between the Higgs boson candidate and the missing transverse momentum, the transverse momentum of the W lepton, the transverse mass of the W boson candidate, the azimuthal separation and the separation in pseudorapidity $\Delta\eta$ between the Higgs boson candidate and the W lepton, the missing transverse momentum, the transverse momentum of the leading jet (if present) and the number of reconstructed jets.

For the four-lepton events the ZH, $H \to \mu\mu$ production is chosen as signal in the BDT training. The variables used in the BDT include the azimuthal separation between the leptons from the $Z \to \ell\ell$ candidate, the azimuthal separation and the separation in pseudorapidity between the $H \to \mu\mu$ candidate and the $Z \to \ell\ell$ candidate, the invariant mass of the $Z \to \ell\ell$ candidate, the number of jets and the transverse momentum of the two leading jets (if present).

Three VH categories are defined by applying selection criteria to the two BDT scores which optimise the sensitivity to the predicted SM signal. Two categories are defined for the three-lepton events and are named VH3LH and VH3LM, where the former has the higher signal-to-background ratio. For the four-lepton events, only one category is selected and is named VH4L. The diboson processes are expected to constitute about 70% (55%) of the total background in the VH3LH (VH3LM) category with smaller contributions expected from top-quark pair production and the DY process. In the VH4L category, about 98% of the background is from the ZZ process. Assuming the SM Higgs boson production and decay, the numbers of signal events expected in the $m_{\mu\mu} = 120$–130 GeV mass window for the VH3LM, VH3LH and VH4L categories are 2.8, 1.4 and 0.5, respectively, and the corresponding signal-to-background ratios are 0.8%, 3.7% and 2.6%. The expected $H \to \mu\mu$ signal purity for the VH production process relative to other Higgs production modes is 89% in the VH3LM category and more than 99% in the VH3LH and VH4L categories.

5.3 *ggF and VBF categories*

The events not selected in the $t\bar{t}H$ or VH categories described above, are further classified according to the number of reconstructed jets into three jet multiplicity categories: 0-jet, 1-jet and 2-jet, where the last includes events with two or more jets. Events with at least one b-tagged jet selected by the 60% efficiency working point or with a third muon with $p_T > 15$ GeV are rejected in the ggF and VBF categories, as they are found to have a very low signal-to-background ratio and negligible signal sensitivity. To fully exploit the kinematic differences between the signal and the backgrounds, which are dominated by DY dimuon production contributing more than 90% of all background events after preselection, BDTs are trained in each jet multiplicity category. All BDTs are trained using the MC background samples and the simulated $H \to \mu\mu$ signal in the mass window $m_{\mu\mu} = 120$–130 GeV.

In the 2-jet category, a BDT is trained to disentangle signal events produced by VBF, used as signal sample in the training, from background events. This BDT, with a score denoted by O_{VBF}, is based on 17 variables related to the dimuon and dijet systems as described below. The dimuon system is characterised by the transverse momentum $p_T^{\mu\mu}$, rapidity $y_{\mu\mu}$ and the value of $\cos\theta^*$. Compared to events from the dominant DY background, signal events from both ggF and VBF production are characterised by larger $p_T^{\mu\mu}$ and smaller absolute values of $y_{\mu\mu}$. The $\cos\theta^*$ distributions provide some discrimination due to different spin-structures and Z–γ interference effects for the DY background [116]. For the leading and subleading jets in the event (denoted by j_1 and j_2), the following variables are computed: p_T and η of j_1 and j_2; the azimuthal separation between the dimuon system and each jet, $\Delta\phi_{\mu\mu,j_1}$ and $\Delta\phi_{\mu\mu,j_2}$; the kinematics of the dijet system (jj) characterised by transverse momentum p_T^{jj}, mass m_{jj} and rapidity y_{jj}; and the azimuthal separation between the dimuon and dijet systems, $\Delta\phi_{\mu\mu,jj}$. These variables exploit the unique signature of the VBF process: two high-p_T jets separated by a large rapidity gap with little hadronic activity. For jets that have a high $p_T > 50$ GeV and are in the central region $|\eta| < 2.1$, the multiplicity of ID tracks with $p_T > 0.5$ GeV associated with each of the two leading jets, N_{track}^{ji}, is also used to help discriminate between jets produced by fragmentation of gluons and quarks [117, 118]. In addition, E_T^{miss} and H_T, which can discriminate the $t\bar{t}$ background from the signal, are also considered.

From the O_{VBF} classifier, four categories in the region with the highest score are selected and named VBF Very High, High, Medium, and Low. The expected $H \to \mu\mu$ signal contributing to these categories is dominated by the VBF process with a purity ranging from about 93% (VBF Very High) to 65% (VBF Low) and the expected SM signal-to-background ratio computed in the 120–130 GeV mass window varies between 18% (VBF Very High) and 2.8% (VBF Low). The predicted number of SM signal events in the VBF categories ranges between 2.8 and 7.5 events.

The remaining events are considered for further classification in three other BDTs split by jet multiplicity, with scores denoted as $O_{ggF}^{(0-2)}$. These BDTs are trained with both the $H \to \mu\mu$ ggF and VBF production MC samples as signal. In each jet category, the same three variables characterising the dimuon system and discussed above are used, i.e. $p_T^{\mu\mu}$, $y_{\mu\mu}$ and $\cos\theta^*$. For the 1-jet BDT, they are complemented by the transverse momentum $p_T^{j_1}$, pseudorapidity η_{j_1}, the track multiplicity $N_{\text{track}}^{j_1}$ in the jet, and the azimuthal separation from the dimuon system, $\Delta\phi_{\mu\mu,j_1}$. In the 2-jet category the same variables as in the VBF BDT are used.

The events in each of these three jet multiplicity categories are further classified into four categories on the basis of the $O_{ggF}^{(0-2)}$ scores to yield a total of 12 mutually exclusive categories called N-jet Very High, High, Medium and Low with $N = 0, 1, 2$. The ggF production process contributes 80%–100% of the expected $H \to \mu\mu$ signal in these categories. The expected SM signal-to-background ratio in the 120–130 GeV

mass window varies from 1.7%–1.5% (2-jet Very High and 1-jet Very High) to 0.07% (0-jet Low). The predicted number of SM signal events in the ggF categories ranges between 17 and 125 events.

6 Signal and background modelling and systematic uncertainties

The signal extraction is based on a binned maximum-likelihood fit to the invariant mass spectrum of the dimuon system as described in Section 7. Analytic models are used in the fit to describe the $m_{\mu\mu}$ distributions for both the signal and background processes.

6.1 Signal modelling

In the SM, the $H \rightarrow \mu\mu$ signal is predicted to be a narrow resonance with a width of 4.1 MeV for $m_H = 125.09$ GeV. The observed signal shape is thus determined by detector resolution effects on the muon momentum measurement. A double-sided Crystal Ball function is used for the Higgs signal model. This function is a modification of the Crystal Ball function [119, 120], and consists of a Gaussian central part with a power-law tail on each side.

For each of the 20 categories, the signal parameters are fitted to signal MC spectra summed over all production modes (ggF, VBF, VH, $t\bar{t}H$) assuming the relative normalisations as predicted by the SM. Within each category no significant differences are found between the signal shapes of the different production modes, indicating that the signal parameterisation is not sensitive to the assumption on their relative normalisations. The width of the Gaussian component of the double-sided Crystal Ball function varies between 2.6 and 3.2 GeV depending on the category. Potential biases in the extracted signal yields due to the analytic parameterisations are tested with a signal injection procedure: in a signal-plus-background fit to pseudo-data constructed from the expected signal and background distributions, the extracted signal yields agree with those injected within the statistical accuracy of about 0.3%.

Several sources of systematic uncertainty in the signal modelling are considered, including both theoretical and experimental effects. The theoretical uncertainties in the signal production affect the number of signal events expected in each category. The uncertainties considered for the main production modes (ggF and VBF) include the impact of the missing higher-order QCD corrections, PDFs, the underlying event and hadronisation. In particular, the uncertainty in the ggF signal is derived using the approach described in Ref. [11], including effects from the variation of QCD scales for factorisation, renormalisation and resummation, and the migration between jet-multiplicity regions [121–128]. The uncertainty in the ggF Higgs boson transverse momentum, including the effect of migration between different kinematic regions and of the treatment of the top-quark mass in the loop corrections, is also taken into account. In addition, dedicated uncertainties are assigned for the ggF signal acceptance in VBF topologies. The uncertainties in the predicted SM branching ratio and Higgs boson production cross sections are included in accord with Ref. [11]. The uncertainties associated with the modelling of the underlying event and parton showering are estimated by considering the PYTHIA 8 systematic eigentune variations and by comparing events showered by PYTHIA 8 with those showered by HERWIG 7 [129, 130]. The impact of the theory uncertainties on the predicted signal acceptances in the different categories ranges between a few per mill and 15% for ggF production. Similarly, for the VBF production the impact of the theory uncertainties on the predicted signal acceptances varies between a few per mill and 7%. For the VH and $t\bar{t}H$ categories the theory systematic

uncertainties have an impact on the predicted signal acceptances of between a few per mill and about 18%.

Systematic uncertainties related to the different reconstructed physics objects used in the analysis affect the expected signal yields in each category. In addition, systematic uncertainties in the muon momentum scale and resolution also affect the signal mass distribution. The experimental uncertainties considered are the muon reconstruction and identification efficiencies, the efficiencies due to the trigger, isolation and impact parameter requirements, the muon momentum scale and resolution [100, 131, 132], the determination of the E_T^{miss} soft term [110], the b-tagging efficiency [109], the uncertainty in the number of tracks associated with the jets [117], the pile-up modelling [90], and uncertainties in the electron reconstruction and identification efficiency [103] as well as in the jet reconstruction efficiency, energy scale and resolution [133]. The impact of the experimental uncertainties on the predicted signal yields and modelling in the different categories is dominated by the uncertainties in the jet energy scale and resolution and the muon momentum resolution. The former can affect signal yields by up to about 10% in some of the 2-jet categories. The muon momentum resolution uncertainty has an impact on the fitted yields ranging between 1% and 6% depending on the category.

The experimental uncertainty of 240 MeV in the assumed value of the Higgs mass from Ref. [5] is also taken into account. All these sources of uncertainty are included in the signal extraction fit described in Section 7 through nuisance parameters acting on the relative signal yields in the different categories and on the signal mass distributions.

6.2 Background modelling

Due to the very small signal-to-background ratio, which is at the level of 0.2% in the region $m_{\mu\mu}$ = 120–130 GeV in an inclusive selection, an accurate determination of the background is of paramount importance. The $m_{\mu\mu}$ background spectrum is parameterised by analytic functions that can describe this distribution at the per-mill level to avoid a significant bias in the extracted signal yields. The mass range used for the fit, $m_{\mu\mu}$ = 110–160 GeV, is optimised to obtain the best signal sensitivity taking into account the statistical and systematic uncertainties.

For the ggF and VBF categories, the background is dominated by the DY process, which accounts for more than 90% of the total, with small contributions from top-quark processes (mainly in the 2-jet categories) and diboson production. In the $t\bar{t}H$ and VH categories, the dominant backgrounds are associated production of $t\bar{t}Z$ and VZ with $Z \rightarrow \mu\mu$, respectively, while the DY process, $t\bar{t}$ production and other diboson processes give minor contributions.

To achieve the required accuracy in the analytic description of the background $m_{\mu\mu}$ distribution, the following approach is used. A *core* function that describes the DY mass shape inclusively is multiplied by an *empirical* function that can correct for distortions of the mass shape due to the event selection and categorisation, higher-order theory corrections and other smaller background contributions. The empirical functions chosen are also flexible enough to describe the background shape in categories where the dominant background is not the DY process. The core function has no free parameters and is common to all categories, while the empirical functions have a certain number of free parameters that are selected and fit to data independently in each category.

The core component of the background is an analytical function based on a LO DY line-shape, described in Appendix A, convoluted with detector effects. The experimental resolution in the dimuon invariant mass is

found to have an important effect on the core function, since it produces a significant shape variation in the mass region just above the Z-boson resonance and thus influences the lower end of the fit region in the $H \to \mu\mu$ search. To take this effect into account, the LO DY line-shape is convolved with a Gaussian function with a mass-dependent resolution derived from the simulation.

The core function is multiplied by the empirical component to obtain the final background parameterisation used in the fits to the $m_{\mu\mu}$ spectra. Two families of functions are studied for this empirical component: power-law functions ('Power') and exponentials of polynomials ('Epoly'), as defined in Table 2.

Table 2: List of tested empirical functional forms for the background modelling.

Function	Expression
PowerN	$m_{\mu\mu}^{(a_0 + a_1 m_{\mu\mu} + a_2 m_{\mu\mu}^2 + ... + a_N m_{\mu\mu}^N)}$
EpolyN	$\exp(a_1 m_{\mu\mu} + a_2 m_{\mu\mu}^2 + ... + a_N m_{\mu\mu}^N)$

The criteria used to select the background functions from among those listed above and to determine the associated systematic uncertainty, referred to as the spurious signal (SS) [1], are described in the following. The SS yields are taken as the measured signals obtained in signal-plus-background fits to the background-only MC templates. They are determined not only for a signal mass of 125 GeV, but also for values of m_H between 120 and 130 GeV in steps of 1 GeV. The templates derived from fast and full simulation DY samples are reweighted using first- or second-order polynomial functions in $m_{\mu\mu}$ to the data sidebands for all these studies.

As a first requirement, only functions able to fit the data sidebands, the fully simulated background samples and the fast DY simulation with a χ^2 probability of the fit greater than 1% (for all these samples) are considered. For the $t\bar{t}H$ and VH categories, only the data sidebands and the fully simulated background samples are considered for these criteria, and the DY contribution is neglected since it is very small and subject to large statistical fluctuations.

For the functions that satisfy these criteria, a spurious-signal test is performed separately in each category. For the ggF and VBF-enriched categories the primary fast-simulation DY sample based on SHERPA as described in Section 3 is used, since it has high statistical precision, while for the $t\bar{t}H$ and the VH categories the fully simulated non-DY background samples are used. Only the functions with the absolute value of the SS below 20% of the expected signal statistical error in data in the mass range 120 to 130 GeV are considered. When applying this requirement, the MC statistical error is subtracted from the absolute value of the SS. Among the functions that pass this requirement, those with the smallest number of degrees of freedom are selected in each category to minimise the statistical uncertainty that dominates in this search. If more than one function per category passes this last selection, the one with the smallest SS is selected. The maximum absolute value of the SS in the mass range 120–130 GeV is taken to be the background modelling uncertainty for the respective category.

As an additional cross-check, the SS tests for the ggF and VBF-enriched categories are also performed on the fully simulated SHERPA DY samples and the alternative fast DY simulation based on the merged POWHEG-BOX and ALPGEN DY samples as explained in Section 3. Further cross-checks are performed with the fast DY simulation after applying several theoretical variations, such as changes of the QCD renormalisation and factorisation scales by factors of two and one half and alternative PDF sets, and experimental variations of the muon momentum resolution and scale and the pile-up jet modelling within the experimental uncertainties. In all these checks, no statistically significant increase in the SS values

is found, hence they are not included as additional systematic uncertainty since their impact would be negligible. The SS systematic uncertainty also addresses any potential local biases in the mass spectra close to the signal region caused by the experimental selections, such as the BDT score requirements or the lepton pairing procedure in the VH categories.

After applying the above criteria, there is no evidence of statistically significant mismodelling, as no SS values are found that are more than two standard deviations away from zero for a signal mass of 125 GeV. This considers the statistical accuracy of the fast DY simulation that is about ten times better than that of the data. All the SS are considered as uncorrelated systematic uncertainties among the different categories. If the SS uncertainties were considered as fully correlated between categories, the expected significance would change by less than 2%.

The SS uncertainties in the different categories range from a few per cent up to about 20% of the expected data statistical uncertainties in the VBF and ggF categories and up to about 30% in the VH and $t\bar{t}H$ categories, which have less statistical precision in their background simulated samples.

6.3 Other systematic uncertainties

In addition to the systematic uncertainties in the signal and background modelling described above, the uncertainty of 1.7% in the combined 2015–2018 integrated luminosity is also considered. It is derived from the calibration of the luminosity scale using x–y beam-separation scans [134], obtained using the LUCID-2 detector [135] for the primary luminosity measurements.

7 Results

The signal yield is obtained by a simultaneous binned maximum-likelihood fit to the $m_{\mu\mu}$ distributions of the 20 categories in the range 110–160 GeV. The chosen bin size is 0.1 GeV. Confidence intervals are based on the profile-likelihood-ratio test statistic [136]. The systematic uncertainties listed in Section 6 are implemented in the fit as nuisance parameters constrained by additional Gaussian or log-normal likelihood terms and the Higgs boson is assumed to have a mass of $m_H = (125.09 \pm 0.24)$ GeV.

The best-fit value of the signal strength parameter, defined as the ratio of the observed signal yield to the one expected in the SM, is $\mu = 1.2 \pm 0.6$, corresponding to an observed (expected) significance of 2.0σ (1.7σ) with respect to the hypothesis of no $H \to \mu\mu$ signal. The spectra of the dimuon invariant mass for all the analysis categories after the signal-plus-background fit are presented in Figure 1. In Figure 1(b) the events are weighted by $\ln(1 + S/B)$, where S are the observed signal yields and B are the background yields derived from the fit to data in the $m_{\mu\mu} = 120$–130 GeV window. These values for S, B and other key quantities are listed in Table 3.

The best-fit values of the signal strength parameters for the five major groups of categories ($t\bar{t}H + VH$, ggF 0-jet, 1-jet, 2-jet, and VBF) are shown in Figure 2 together with the combined value. A goodness-of-fit test is performed using the saturated model technique [137] and returns a probability of 10%.

The signal strength uncertainty is dominated by the data statistical error of about ± 0.58. The impact of the systematic uncertainties on the signal strength is found to be $^{+0.18}_{-0.13}$, with contributions from the signal theory uncertainties that account for $^{+0.13}_{-0.08}$, the signal experimental uncertainties that account for $^{+0.07}_{-0.03}$ and the spurious-signal uncertainties that account for ± 0.10.
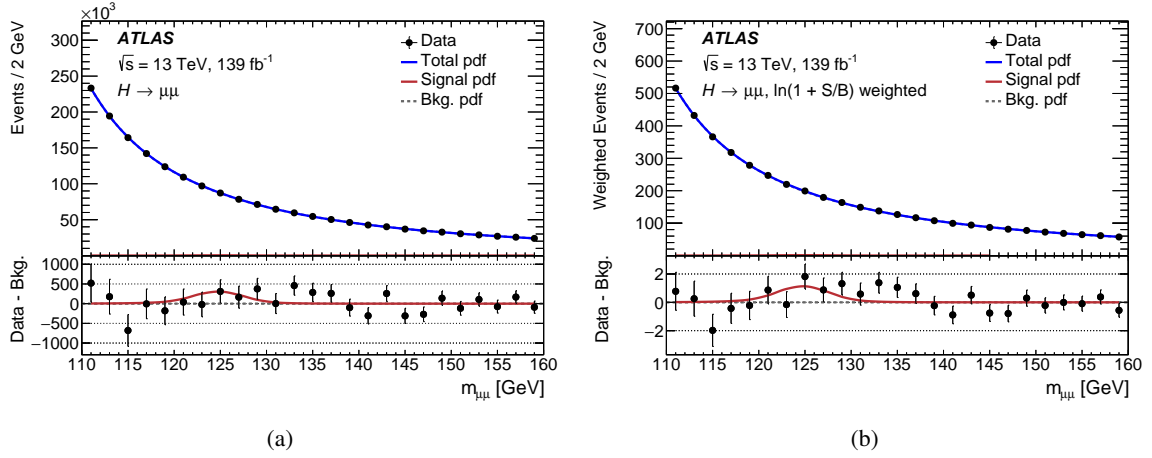
Figure 1: Dimuon invariant mass spectrum in all the analysis categories observed in data. In (a) the unweighted sum of all events and signal plus background probability density functions (pdf) are shown, while in (b) events and pdfs are weighted by $\ln(1 + S/B)$, where S are the observed signal yields and B are the background yields derived from the fit to data in the $m_{\mu\mu} = 120$–130 GeV window. The background and signal pdf are derived from the fit to the data, with S normalised to its best-fit value. The lower panels compare the fitted signal pdf, normalised to the signal best-fit value, to the difference between the data and the background model. The error bars represent the data statistical uncertainties.
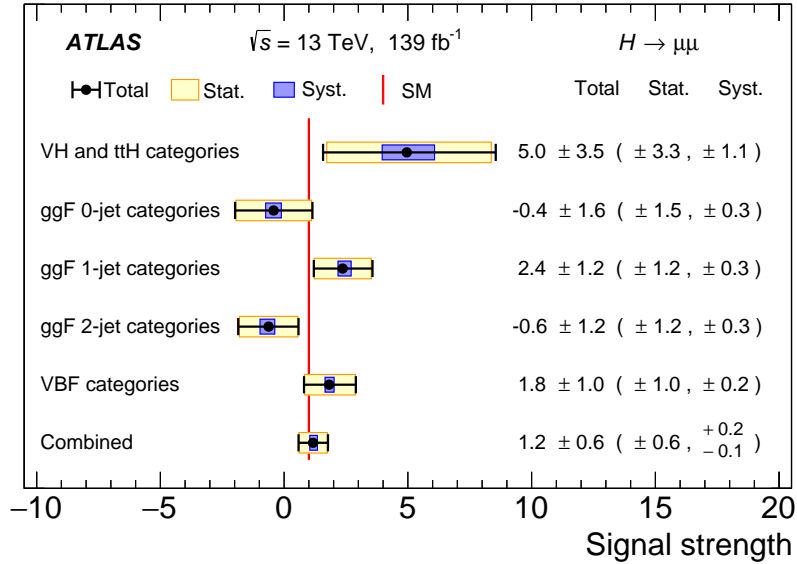

Figure 2: The best-fit values of the signal strength parameters for the five major groups of categories ($t\bar{t}H$ +VH, ggF 0-jet, 1-jet, 2-jet, and VBF) together with the combined value.

Table 3: Number of events observed in the $m_{\mu\mu} = 120$–130 GeV window in data, the number of signal events expected in the SM (S_{SM}), and events from signal ($S = \mu \times S_{\mathrm{SM}}$) and background ($B$) as derived from the combined fit to the data with a signal strength parameter of $\mu = 1.2$. The uncertainties in S_{SM} correspond to the systematic uncertainty of the SM prediction, the uncertainty in S is given by that in μ, and the uncertainty in B is given by the sum in quadrature of the statistical uncertainty from the fit and the SS uncertainty. In addition the observed number of signal events divided by the square root of the number of background events ($S/\sqrt{B}$) and the signal-to-background ratio (S/B) in % for each of the 20 categories described in the text are displayed. In the last column, the width of the Gaussian component of the double-sided Crystal Ball function used in the signal modelling (σ, as described in Section 6) is reported.

Category	Data	S_{SM}	S	B	$S/\sqrt{B}$	S/B [%]	σ [GeV]
VBF Very High	15	2.81 ± 0.27	3.3 ± 1.7	14.5 ± 2.1	0.86	22.6	3.0
VBF High	39	3.46 ± 0.36	4.0 ± 2.1	32.5 ± 2.9	0.71	12.4	3.0
VBF Medium	112	4.8 ± 0.5	5.6 ± 2.8	85 ± 4	0.61	6.6	2.9
VBF Low	284	7.5 ± 0.9	9 ± 4	273 ± 8	0.53	3.2	3.0
2-jet Very High	1030	17.6 ± 3.3	21 ± 10	1024 ± 22	0.63	2.0	3.1
2-jet High	5433	50 ± 8	58 ± 30	5440 ± 50	0.77	1.0	2.9
2-jet Medium	18 311	79 ± 15	90 ± 50	$18\,320 \pm 90$	0.66	0.5	2.9
2-jet Low	36 409	63 ± 17	70 ± 40	$36\,340 \pm 140$	0.37	0.2	2.9
1-jet Very High	1097	16.5 ± 2.4	19 ± 10	1071 ± 22	0.59	1.8	2.9
1-jet High	6413	46 ± 7	54 ± 28	6320 ± 50	0.69	0.9	2.8
1-jet Medium	24 576	90 ± 11	100 ± 50	$24\,290 \pm 100$	0.67	0.4	2.7
1-jet Low	73 459	125 ± 17	150 ± 70	$73\,480 \pm 190$	0.53	0.2	2.8
0-jet Very High	15 986	59 ± 11	70 ± 40	$16\,090 \pm 90$	0.55	0.4	2.6
0-jet High	46 523	99 ± 13	120 ± 60	$46\,190 \pm 150$	0.54	0.3	2.6
0-jet Medium	91 392	119 ± 14	140 ± 70	$91\,310 \pm 210$	0.46	0.2	2.7
0-jet Low	121 354	79 ± 10	90 ± 50	$121\,310 \pm 280$	0.26	0.1	2.7
VH4L	34	0.53 ± 0.05	0.6 ± 0.3	24 ± 4	0.13	2.6	2.9
VH3LH	41	1.45 ± 0.14	1.7 ± 0.9	41 ± 5	0.27	4.2	3.1
VH3LM	358	2.76 ± 0.24	3.2 ± 1.6	347 ± 15	0.17	0.9	3.0
$t\bar{t}H$	17	1.19 ± 0.13	1.4 ± 0.7	15.1 ± 2.2	0.36	9.2	3.2

The compatibility of the measured signal strengths between the 20 categories is tested by repeating the fit after allowing each category to have its own signal strength parameter. The probability of compatibility is found to be at the level of 2%. With the same methodology, the probability of compatibility between the signal strengths of the five groups of categories shown in Figure 2 is found to be 20%. Among the 20 categories, those with an individual signal strength at the level of two standard deviations from the mean value are the VBF Medium, the 0-jet Very High and the VH4L. For each of these three categories, it was checked that adding one degree of freedom to the function used to model the background or changing the functional form from 'Power' to 'Epoly' does not significantly impact the analysis results or the probability of compatibility between the 20 categories.

An upper limit on the signal strength μ is computed using a modified frequentist $\mathrm{CL_s}$ method [136, 138]. The observed upper limit on μ at 95% confidence level (CL) is found to be 2.2, with an expected limit of 1.1 for the case of no $H \rightarrow \mu\mu$ signal and an expected limit of 2.0 for the case of an $H \rightarrow \mu\mu$ signal at SM strength. The corresponding branching ratio upper limit at 95% CL is $B(H \rightarrow \mu\mu) < 4.7 \cdot 10^{-4}$, assuming the SM cross section for Higgs boson production.

This result represents an improvement of about a factor of 2.5 in expected sensitivity compared with the previous ATLAS publication [14]. Of this improvement, a factor of about two is due to the larger analysed

dataset and the additional 25% improvement can be attributed to more advanced analysis techniques.

8 Conclusion

A search for the rare dimuon decay of the Higgs boson is performed using the full Run 2 dataset of 139 fb^{-1} collected with the ATLAS detector in pp collisions at $\sqrt{s} = 13$ TeV at the LHC. The best-fit value for the SM $H \to \mu\mu$ signal strength parameter is found to be $\mu = 1.2 \pm 0.6$, corresponding to an observed (expected) significance of 2.0σ (1.7σ) with respect to the hypothesis of no $H \to \mu\mu$ signal. An upper limit of 2.2 at 95% CL is set on the signal strength, while 1.1 is expected for the case of no $H \to \mu\mu$ signal.

Acknowledgements

A Expression for the leading-order Drell–Yan lineshape

The core component of the background function is based on a LO DY line-shape (see e.g. Ref. [116]):

$$DY(m_{\mu\mu}) = \sum_q \mathcal{L}_{q\bar{q}}(m_{\mu\mu}) \cdot \sigma_{q\bar{q}}(m_{\mu\mu}) , \quad q = u, \ s, \ d .$$

The parton luminosity contribution $\mathcal{L}_{q\bar{q}}$ is derived from the PDF4LHC15 PDF set as a function of $\hat{s} = m_{\mu\mu}^2$ using APFEL [140] interfaced to LHAPDF [141] and parameterised using a 6th order polynomial. The matrix element component $\sigma_{q\bar{q}}(\hat{s}) = \sigma_{q\bar{q}}(m_{\mu\mu})/(2m_{\mu\mu})$ can be expressed as

$$\sigma_{q\bar{q}}(\hat{s}) = \frac{4\pi\alpha^2}{3\hat{s}N_c}[Q_q^2 - 2Q_q V_\ell V_q \chi_{Z\gamma}(\hat{s}) + (A_\ell^2 + V_\ell^2)(A_q^2 + V_q^2)\chi_Z(\hat{s})] ,$$

where

$$\chi_{Z\gamma}(\hat{s}) = \kappa \frac{\hat{s}(\hat{s} - m_Z^2)}{(\hat{s} - m_Z^2)^2 + \Gamma_Z^2 m_Z^2} ,$$

$$\chi_Z(\hat{s}) = \kappa^2 \frac{\hat{s}^2}{(\hat{s} - m_Z^2)^2 + \Gamma_Z^2 m_Z^2} ,$$

$$\kappa = \frac{\sqrt{2}G_F m_Z^2}{4\pi\alpha} .$$

Here Q, V, A denote the electric charges, vector and axial-vector couplings of the fermions, α, G_F the electroweak couplings, m_Z, Γ_Z the mass and width of the Z-boson using values from Ref. [142] and $N_c = 3$ the number of QCD colour charges. The DY function described above is then convolved with a Gaussian function with a mass-dependent resolution derived from the simulation.

References

[1] ATLAS Collaboration, *Observation of a new particle in the search for the Standard Model Higgs boson with the ATLAS detector at the LHC*, Phys. Lett. B **716** (2012) 1, arXiv: 1207.7214 [hep-ex].

[2] CMS Collaboration, *Observation of a new boson at a mass of 125 GeV with the CMS experiment at the LHC*, Phys. Lett. B **716** (2012) 30, arXiv: 1207.7235 [hep-ex].

[3] ATLAS Collaboration, *Study of the spin and parity of the Higgs boson in diboson decays with the ATLAS detector*, Eur. Phys. J. C **75** (2015) 476, arXiv: 1506.05669 [hep-ex], Erratum: Eur. Phys. J. C **76** (2016) 152.

[4] CMS Collaboration, *Constraints on the spin-parity and anomalous HVV couplings of the Higgs boson in proton collisions at 7 and 8 TeV*, Phys. Rev. D **92** (2015) 012004, arXiv: 1411.3441 [hep-ex].

[5] ATLAS and CMS Collaborations, *Combined Measurement of the Higgs Boson Mass in pp Collisions at $\sqrt{s} = 7$ and 8 TeV with the ATLAS and CMS Experiments*, Phys. Rev. Lett. **114** (2015) 191803, arXiv: 1503.07589 [hep-ex].

[6] ATLAS and CMS Collaborations, *Measurements of the Higgs boson production and decay rates and constraints on its couplings from a combined ATLAS and CMS analysis of the LHC pp collision data at $\sqrt{s} = 7$ and 8 TeV*, JHEP **08** (2016) 045, arXiv: 1606.02266 [hep-ex].

[7] ATLAS Collaboration, *Observation of $H \to b\bar{b}$ decays and VH production with the ATLAS detector*, Phys. Lett. B **786** (2018) 59, arXiv: 1808.08238 [hep-ex].

[8] ATLAS Collaboration, *Observation of Higgs boson production in association with a top quark pair at the LHC with the ATLAS detector*, Phys. Lett. B **784** (2018) 173, arXiv: 1806.00425 [hep-ex].

[9] CMS Collaboration, *Observation of Higgs Boson Decay to Bottom Quarks*, Phys. Rev. Lett. **121** (2018) 121801, arXiv: 1808.08242 [hep-ex].

[10] CMS Collaboration, *Observation of $t\bar{t}H$ Production*, Phys. Rev. Lett. **120** (2018) 231801, arXiv: 1804.02610 [hep-ex].

[11] LHC Higgs Cross Section Working Group, D. de Florian, C. Grojean, F. Maltoni, C. Mariotti, A. Nikitenko, M. Pieri, P. Savard, M. Schumacher, R. Tanaka (Eds.), *Handbook of LHC Higgs cross sections: 4. Deciphering the nature of the Higgs sector*, CYRM-2017-002 (2016), arXiv: 1610.07922 [hep-ph].

[12] N. Vignaroli, *Searching for a dilaton decaying to muon pairs at the LHC*, Phys. Rev. D **80** (2009) 095023, arXiv: 0906.4078 [hep-ph].

[13] A. Dery, A. Efrati, Y. Hochberg and Y. Nir, *What if $BR(h \to \mu\mu)/BR(h \to \tau\tau) \neq m_\mu^2/m_\tau^2$?*, JHEP **05** (2013) 039, arXiv: 1302.3229 [hep-ph].

[14] ATLAS Collaboration, *Search for the Dimuon Decay of the Higgs Boson in pp Collisions at $\sqrt{s} = 13$ TeV with the ATLAS Detector*, Phys. Rev. Lett. **119** (2017) 051802, arXiv: 1705.04582 [hep-ex].

[15] CMS Collaboration, *Search for the Higgs Boson Decaying to Two Muons in Proton–Proton Collisions at $\sqrt{s} = 13$ TeV*, Phys. Rev. Lett. **122** (2019) 021801, arXiv: 1807.06325 [hep-ex].

[16] ATLAS Collaboration, *Measurement of the Higgs boson mass in the $H \to ZZ^* \to 4\ell$ and $H \to \gamma\gamma$ channels with $\sqrt{s} = 13$ TeV pp collisions using the ATLAS detector*, Phys. Lett. B **784** (2018) 345, arXiv: 1806.00242 [hep-ex].

[17] CMS Collaboration, *A measurement of the Higgs boson mass in the diphoton decay channel*, Phys. Lett. B **805** (2020) 135425, arXiv: 2002.06398 [hep-ex].

[18] ATLAS Collaboration, *The ATLAS Experiment at the CERN Large Hadron Collider*, JINST **3** (2008) S08003.

[19] ATLAS Collaboration, *ATLAS Insertable B-Layer: Technical Design Report*, ATLAS-TDR-19; CERN-LHCC-2010-013, 2010, URL: https://cds.cern.ch/record/1291633.

[20] ATLAS Collaboration, *Performance of the ATLAS trigger system in 2015*, Eur. Phys. J. C **77** (2017) 317, arXiv: 1611.09661 [hep-ex].

[21] ATLAS Collaboration, *The ATLAS Simulation Infrastructure*, Eur. Phys. J. C **70** (2010) 823, arXiv: 1005.4568 [physics.ins-det].

[22] S. Agostinelli et al., *GEANT4: a simulation toolkit*, Nucl. Instrum. Meth. A **506** (2003) 250.

[23] LHC Higgs Cross Section Working Group, S. Heinemeyer, C. Mariotti, G. Passarino and R. Tanaka (Eds.), *Handbook of LHC Higgs Cross Sections: 3. Higgs Properties*, CERN-2013-004 (2013), arXiv: 1307.1347 [hep-ph].

[24] A. Djouadi, J. Kalinowski and M. Spira, *HDECAY: A program for Higgs boson decays in the Standard Model and its supersymmetric extension*, Comput. Phys. Commun. **108** (1998) 56, arXiv: hep-ph/9704448.

[25] M. Spira, *QCD Effects in Higgs Physics*, Fortsch. Phys. **46** (1998) 203, arXiv: hep-ph/9705337.

[26] A. Djouadi, M. M. Mühlleitner and M. Spira, *Decays of supersymmetric particles: The Program SUSY-HIT (SUspect-SdecaY-Hdecay-InTerface)*, Acta Phys. Polon. B **38** (2007) 635, arXiv: hep-ph/0609292.

[27] A. Djouadi, J. Kalinowski, M. Mühlleitner and M. Spira, *HDECAY: Twenty++ years after*, Computer Physics Communications **238** (2019) 214, ISSN: 0010-4655, URL: http://dx.doi.org/10.1016/j.cpc.2018.12.010.

[28] A. Bredenstein, A. Denner, S. Dittmaier and M. M. Weber, *Radiative corrections to the semileptonic and hadronic Higgs-boson decays $H \rightarrow WW/ZZ \rightarrow 4$ fermions*, JHEP **02** (2007) 080, arXiv: hep-ph/0611234.

[29] A. Bredenstein, A. Denner, S. Dittmaier and M. M. Weber, *Precise predictions for the Higgs-boson decay $H \rightarrow WW/ZZ \rightarrow 4$ leptons*, Phys. Rev. D **74** (2006) 013004, arXiv: hep-ph/0604011.

[30] A. Bredenstein, A. Denner, S. Dittmaier and M. M. Weber, *Precision calculations for the Higgs decays $H \rightarrow ZZ/WW \rightarrow 4$ leptons*, Nucl. Phys. Proc. Suppl. **160** (2006) 131, arXiv: hep-ph/0607060.

[31] P. Nason, *A New method for combining NLO QCD with shower Monte Carlo algorithms*, JHEP **11** (2004) 040, arXiv: hep-ph/0409146.

[32] S. Frixione, P. Nason and C. Oleari, *Matching NLO QCD computations with parton shower simulations: the POWHEG method*, JHEP **11** (2007) 070, arXiv: 0709.2092 [hep-ph].

[33] S. Alioli, P. Nason, C. Oleari and E. Re, *A general framework for implementing NLO calculations in shower Monte Carlo programs: the POWHEG BOX*, JHEP **06** (2010) 043, arXiv: 1002.2581 [hep-ph].

[34] J. M. Campbell et al., *NLO Higgs boson production plus one and two jets using the POWHEG BOX, MadGraph4 and MCFM*, JHEP **07** (2012) 092, arXiv: 1202.5475 [hep-ph].

[35] K. Hamilton, P. Nason and G. Zanderighi, *MINLO: multi-scale improved NLO*, JHEP **10** (2012) 155, arXiv: 1206.3572 [hep-ph].

[36] K. Hamilton, P. Nason, C. Oleari and G. Zanderighi, *Merging H/W/Z + 0 and 1 jet at NLO with no merging scale: a path to parton shower + NNLO matching*, JHEP **05** (2013) 082, arXiv: 1212.4504 [hep-ph].

[37] K. Hamilton, P. Nason, E. Re and G. Zanderighi, *NNLOPS simulation of Higgs boson production*, JHEP **10** (2013) 222, arXiv: `1309.0017 [hep-ph]`.

[38] K. Hamilton, P. Nason and G. Zanderighi,
Finite quark-mass effects in the NNLOPS POWHEG+MiNLO Higgs generator,
JHEP **05** (2015) 140, arXiv: `1501.04637 [hep-ph]`.

[39] J. Butterworth et al., *PDF4LHC recommendations for LHC Run II*, J. Phys. G **43** (2016) 023001,
arXiv: `1510.03865 [hep-ph]`.

[40] S. Catani and M. Grazzini, *Next-to-Next-to-Leading-Order Subtraction Formalism in Hadron
Collisions and its Application to Higgs-Boson Production at the Large Hadron Collider*,
Phys. Rev. Lett. **98** (2007) 222002, arXiv: `hep-ph/0703012`.

[41] T. Sjöstrand et al., *An introduction to PYTHIA 8.2*, Comput. Phys. Commun. **191** (2015) 159,
arXiv: `1410.3012 [hep-ph]`.

[42] ATLAS Collaboration, *Measurement of the Z/γ^* boson transverse momentum distribution in pp
collisions at $\sqrt{s} = 7$ TeV with the ATLAS detector*, JHEP **09** (2014) 145,
arXiv: `1406.3660 [hep-ex]`.

[43] U. Aglietti, R. Bonciani, G. Degrassi and A. Vicini,
Two-loop light fermion contribution to Higgs production and decays, Phys. Lett. B **595** (2004) 432,
arXiv: `hep-ph/0404071`.

[44] S. Actis, G. Passarino, C. Sturm and S. Uccirati,
NLO electroweak corrections to Higgs boson production at hadron colliders,
Phys. Lett. B **670** (2008) 12, arXiv: `0809.1301 [hep-ph]`.

[45] S. Actis, G. Passarino, C. Sturm and S. Uccirati,
NNLO computational techniques: The cases $H \to \gamma\gamma$ and $H \to gg$, Nucl. Phys. B **811** (2009) 182,
arXiv: `0809.3667 [hep-ph]`.

[46] C. Anastasiou, R. Boughezal and F. Petriello,
Mixed QCD-electroweak corrections to Higgs boson production in gluon fusion,
JHEP **04** (2009) 003, arXiv: `0811.3458 [hep-ph]`.

[47] A. Pak, M. Rogal and M. Steinhauser,
Finite top quark mass effects in NNLO Higgs boson production at LHC, JHEP **02** (2010) 025,
arXiv: `0911.4662 [hep-ph]`.

[48] R. V. Harlander and K. J. Ozeren,
Top mass effects in Higgs production at next-to-next-to-leading order QCD: Virtual corrections,
Phys. Lett. B **679** (2009) 467, arXiv: `0907.2997 [hep-ph]`.

[49] R. V. Harlander and K. J. Ozeren,
Finite top mass effects for hadronic Higgs production at next-to-next-to-leading order,
JHEP **11** (2009) 088, arXiv: `0909.3420 [hep-ph]`.

[50] R. V. Harlander, H. Mantler, S. Marzani and K. J. Ozeren,
Higgs production in gluon fusion at next-to-next-to-leading order QCD for finite top mass,
Eur. Phys. J. C **66** (2010) 359, arXiv: `0912.2104 [hep-ph]`.

[51] C. Anastasiou, C. Duhr, F. Dulat, F. Herzog and B. Mistlberger,
Higgs Boson Gluon-Fusion Production in QCD at Three Loops,
Phys. Rev. Lett. **114** (2015) 212001, arXiv: `1503.06056 [hep-ph]`.

[52] C. Anastasiou et al.,
High precision determination of the gluon fusion Higgs boson cross-section at the LHC,
JHEP **05** (2016) 058, arXiv: 1602.00695 [hep-ph].

[53] F. Dulat, A. Lazopoulos and B. Mistlberger, *iHixs 2 – Inclusive Higgs cross sections*,
Comput. Phys. Commun. **233** (2018) 243, arXiv: 1802.00827 [hep-ph].

[54] M. Bonetti, K. Melnikov and L. Tancredi, *Higher order corrections to mixed QCD-EW
contributions to Higgs boson production in gluon fusion*,
Phys. Rev. D **97** (2018) 056017, [Erratum: Phys. Rev. D 97 (2018) 099906],
arXiv: 1801.10403 [hep-ph].

[55] P. Nason and C. Oleari,
NLO Higgs boson production via vector-boson fusion matched with shower in POWHEG,
JHEP **02** (2010) 037, arXiv: 0911.5299 [hep-ph].

[56] G. Cullen et al., *Automated one-loop calculations with GoSam*, Eur. Phys. J. C **72** (2012) 1889,
arXiv: 1111.2034 [hep-ph].

[57] G. Luisoni, P. Nason, C. Oleari and F. Tramontano, *HW$^\pm$/HZ + 0 and 1 jet at NLO with the
POWHEG BOX interfaced to GoSam and their merging within MiNLO*, JHEP **10** (2013) 083,
arXiv: 1306.2542 [hep-ph].

[58] M. Ciccolini, A. Denner and S. Dittmaier, *Strong and Electroweak Corrections to the Production
of Higgs + 2 Jets via Weak Interactions at the Large Hadron Collider*,
Phys. Rev. Lett. **99** (2007) 161803, arXiv: 0707.0381 [hep-ph].

[59] M. Ciccolini, A. Denner and S. Dittmaier,
Electroweak and QCD corrections to Higgs production via vector-boson fusion at the CERN LHC,
Phys. Rev. D **77** (2008) 013002, arXiv: 0710.4749 [hep-ph].

[60] P. Bolzoni, F. Maltoni, S.-O. Moch and M. Zaro,
Higgs Boson Production via Vector-Boson Fusion at Next-to-Next-to-Leading Order in QCD,
Phys. Rev. Lett. **105** (2010) 011801, arXiv: 1003.4451 [hep-ph].

[61] M. L. Ciccolini, S. Dittmaier and M. Krämer,
Electroweak radiative corrections to associated WH and ZH production at hadron colliders,
Phys. Rev. D **68** (2003) 073003, arXiv: hep-ph/0306234 [hep-ph].

[62] O. Brein, A. Djouadi and R. Harlander,
NNLO QCD corrections to the Higgs-strahlung processes at hadron colliders,
Phys. Lett. B **579** (2004) 149, arXiv: hep-ph/0307206.

[63] O. Brein, R. Harlander, M. Wiesemann and T. Zirke,
Top-quark mediated effects in hadronic Higgs-Strahlung, Eur. Phys. J. C **72** (2012) 1868,
arXiv: 1111.0761 [hep-ph].

[64] L. Altenkamp, S. Dittmaier, R. V. Harlander, H. Rzehak and T. J. E. Zirke,
Gluon-induced Higgs-strahlung at next-to-leading order QCD, JHEP **02** (2013) 078,
arXiv: 1211.5015 [hep-ph].

[65] A. Denner, S. Dittmaier, S. Kallweit and A. Mück, *HAWK 2.0: A Monte Carlo program for Higgs
production in vector-boson fusion and Higgs strahlung at hadron colliders*,
Comput. Phys. Commun. **195** (2015) 161, arXiv: 1412.5390 [hep-ph].

[66] O. Brein, R. V. Harlander and T. J. E. Zirke, *vh@nnlo – Higgs Strahlung at hadron colliders*,
Comput. Phys. Commun. **184** (2013) 998, arXiv: 1210.5347 [hep-ph].

[67] R. V. Harlander, A. Kulesza, V. Theeuwes and T. Zirke,
Soft gluon resummation for gluon-induced Higgs Strahlung, JHEP **11** (2014) 082,
arXiv: 1410.0217 [hep-ph].

[68] R. V. Harlander, J. Klappert, S. Liebler and L. Simon,
vh@nnlo-v2: new physics in Higgs Strahlung, JHEP **05** (2018) 089,
arXiv: 1802.04817 [hep-ph].

[69] J. Alwall et al., *The automated computation of tree-level and next-to-leading order differential
cross sections, and their matching to parton shower simulations*, JHEP **07** (2014) 079,
arXiv: 1405.0301 [hep-ph].

[70] P. Artoisenet, R. Frederix, O. Mattelaer and R. Rietkerk,
Automatic spin-entangled decays of heavy resonances in Monte Carlo simulations,
JHEP **03** (2013) 015, arXiv: 1212.3460 [hep-ph].

[71] R. D. Ball et al., *Parton distributions for the LHC run II*, JHEP **04** (2015) 040,
arXiv: 1410.8849 [hep-ph].

[72] ATLAS Collaboration, *ATLAS Pythia 8 tunes to 7 TeV data*, ATL-PHYS-PUB-2014-021, 2014,
URL: https://cds.cern.ch/record/1966419.

[73] W. Beenakker et al., *NLO QCD corrections to $t\bar{t}H$ production in hadron collisions*,
Nucl. Phys. B **653** (2003) 151, arXiv: hep-ph/0211352.

[74] S. Dawson, C. Jackson, L. H. Orr, L. Reina and D. Wackeroth, *Associated Higgs boson production
with top quarks at the CERN Large Hadron Collider: NLO QCD corrections*,
Phys. Rev. D **68** (2003) 034022, arXiv: hep-ph/0305087.

[75] Y. Zhang, W.-G. Ma, R.-Y. Zhang, C. Chen and L. Guo,
QCD NLO and EW NLO corrections to $t\bar{t}H$ production with top quark decays at hadron collider,
Phys. Lett. B **738** (2014) 1, arXiv: 1407.1110 [hep-ph].

[76] S. Frixione, V. Hirschi, D. Pagani, H.-S. Shao and M. Zaro,
Electroweak and QCD corrections to top-pair hadroproduction in association with heavy bosons,
JHEP **06** (2015) 184, arXiv: 1504.03446 [hep-ph].

[77] E. Bothmann et al., *Event Generation with Sherpa 2.2*, SciPost Phys. **7** (2019) 034,
arXiv: 1905.09127 [hep-ph].

[78] T. Gleisberg and S. Höche, *Comix, a new matrix element generator*, JHEP **12** (2008) 039,
arXiv: 0808.3674 [hep-ph].

[79] F. Cascioli, P. Maierhofer and S. Pozzorini, *Scattering Amplitudes with Open Loops*,
Phys. Rev. Lett. **108** (2012) 111601, arXiv: 1111.5206 [hep-ph].

[80] A. Denner, S. Dittmaier and L. Hofer,
Collier: A fortran-based complex one-loop library in extended regularizations,
Comput. Phys. Commun. **212** (2017) 220, arXiv: 1604.06792 [hep-ph].

[81] S. Schumann and F. Krauss,
A Parton shower algorithm based on Catani-Seymour dipole factorisation, JHEP **03** (2008) 038,
arXiv: 0709.1027 [hep-ph].

[82] S. Höche, F. Krauss, M. Schönherr and F. Siegert,
A critical appraisal of NLO+PS matching methods, JHEP **09** (2012) 049,
arXiv: 1111.1220 [hep-ph].

[83] S. Höche, F. Krauss, M. Schönherr and F. Siegert,
QCD matrix elements + parton showers: The NLO case, JHEP **04** (2013) 027,
arXiv: 1207.5030 [hep-ph].

[84] S. Catani, F. Krauss, R. Kuhn and B. R. Webber, *QCD Matrix Elements + Parton Showers*,
JHEP **11** (2001) 063, arXiv: hep-ph/0109231.

[85] S. Höche, F. Krauss, S. Schumann and F. Siegert, *QCD matrix elements and truncated showers*,
JHEP **05** (2009) 053, arXiv: 0903.1219 [hep-ph].

[86] S. Frixione, P. Nason and G. Ridolfi,
A Positive-weight next-to-leading-order Monte Carlo for heavy flavour hadroproduction,
JHEP **09** (2007) 126, arXiv: 0707.3088 [hep-ph].

[87] E. Re,
Single-top Wt-channel production matched with parton showers using the POWHEG method,
Eur. Phys. J. C **71** (2011) 1547, arXiv: 1009.2450 [hep-ph].

[88] S. Frixione, E. Laenen, P. Motylinski, C. D. White and B. R. Webber,
Single-top hadroproduction in association with a W boson, JHEP **07** (2008) 029,
arXiv: 0805.3067 [hep-ph].

[89] R. D. Ball et al., *Parton distributions with LHC data*, Nucl. Phys. B **867** (2013) 244,
arXiv: 1207.1303 [hep-ph].

[90] ATLAS Collaboration, *The Pythia 8 A3 tune description of ATLAS minimum bias and inelastic
measurements incorporating the Donnachie–Landshoff diffractive model*,
ATL-PHYS-PUB-2016-017, 2016, URL: https://cds.cern.ch/record/2206965.

[91] Work supported by the U.S. Scientific Discovery through Advanced Computing (SciDAC)
program, grant "HEP Data Analytics on HPC" No. 1013935.

[92] S. Höche, S. Prestel and H. Schulz,
Simulation of vector boson plus many jet final states at the high luminosity LHC,
Phys. Rev. D **100** (2019) 014024, arXiv: 1905.05120 [hep-ph].

[93] S. Dulat et al.,
New parton distribution functions from a global analysis of quantum chromodynamics,
Phys. Rev. D **93** (2016) 033006, arXiv: 1506.07443 [hep-ph].

[94] L. Lönnblad, *Correcting the Colour-Dipole Cascade Model with Fixed Order Matrix Elements*,
JHEP **05** (2002) 046, arXiv: hep-ph/0112284 [hep-ph].

[95] L. Barze et al.,
Neutral current Drell-Yan with combined QCD and electroweak corrections in the POWHEG BOX,
Eur. Phys. J. C **73** (2013) 2474, arXiv: 1302.4606 [hep-ph].

[96] H.-L. Lai et al., *New parton distributions for collider physics*, Phys. Rev. D **82** (2010) 074024,
arXiv: 1007.2241 [hep-ph].

[97] M. L. Mangano et al., *ALPGEN, a generator for hard multiparton processes in hadronic collisions*,
JHEP **07** (2003) 001, arXiv: hep-ph/0206293.

[98] J. Pumplin et al.,
New Generation of Parton Distributions with Uncertainties from Global QCD Analysis,
JHEP **07** (2002) 012, arXiv: hep-ph/0201195.

[99] P. Golonka and Z. Was, *Next-to-leading logarithms and the PHOTOS Monte Carlo*,
Eur. Phys. J. C **50** (2007) 53, arXiv: `hep-ph/0604232 [hep-ph]`.

[100] ATLAS Collaboration, *Muon reconstruction and identification efficiency in ATLAS using the full Run 2 pp collision data set at $\sqrt{s}$ = 13 TeV*, (2020), arXiv: `2012.00578 [hep-ex]`.

[101] ATLAS Collaboration, *Higgs boson production cross-section measurements and their EFT interpretation in the 4ℓ decay channel at $\sqrt{s}$ = 13 TeV with the ATLAS detector*,
Eur. Phys. J. C **80** (2020) 957, arXiv: `2004.03447 [hep-ex]`.

[102] ATLAS Collaboration, *A search for the $Z\gamma$ decay mode of the Higgs boson in pp collisions at $\sqrt{s}$ = 13 TeV with the ATLAS detector*, Phys. Lett. B **809** (2020) 135754,
arXiv: `2005.05382 [hep-ex]`.

[103] ATLAS Collaboration, *Electron and photon performance measurements with the ATLAS detector using the 2015–2017 LHC proton–proton collision data*, JINST **14** (2019) P12006,
arXiv: `1908.00005 [hep-ex]`.

[104] ATLAS Collaboration,
Jet reconstruction and performance using particle flow with the ATLAS Detector,
Eur. Phys. J. C **77** (2017) 466, arXiv: `1703.10485 [hep-ex]`.

[105] M. Cacciari, G. P. Salam and G. Soyez, *The anti-k_t jet clustering algorithm*, JHEP **04** (2008) 063,
arXiv: `0802.1189 [hep-ph]`.

[106] M. Cacciari, G. P. Salam and G. Soyez, *FastJet user manual*, Eur. Phys. J. C **72** (2012) 1896,
arXiv: `1111.6097 [hep-ph]`.

[107] ATLAS Collaboration, *Performance of pile-up mitigation techniques for jets in pp collisions at $\sqrt{s}$ = 8 TeV using the ATLAS detector*, Eur. Phys. J. C **76** (2016) 581,
arXiv: `1510.03823 [hep-ex]`.

[108] ATLAS Collaboration,
Measurements of b-jet tagging efficiency with the ATLAS detector using $t\bar{t}$ events at $\sqrt{s}$ = 13 TeV,
JHEP **08** (2018) 089, arXiv: `1805.01845 [hep-ex]`.

[109] ATLAS Collaboration, *ATLAS b-jet identification performance and efficiency measurement with $t\bar{t}$ events in pp collisions at $\sqrt{s}$ = 13 TeV*, Eur. Phys. J. C **79** (2019) 970,
arXiv: `1907.05120 [hep-ex]`.

[110] ATLAS Collaboration, *Performance of missing transverse momentum reconstruction with the ATLAS detector using proton–proton collisions at $\sqrt{s}$ = 13 TeV*, Eur. Phys. J. C **78** (2018) 903,
arXiv: `1802.08168 [hep-ex]`.

[111] ATLAS Collaboration,
E_T^{miss} performance in the ATLAS detector using 2015–2016 LHC pp collisions,
ATLAS-CONF-2018-023, 2018, URL: `https://cds.cern.ch/record/2625233`.

[112] L. Breiman, J. Friedman, R. Olshen and C. Stone, *Classification and Regression Trees*,
Wadsworth and Brooks, 1984.

[113] B. P. Roe et al., *Boosted decision trees, an alternative to artificial neural networks*,
Nucl. Instrum. Meth. A **543** (2005) 577, arXiv: `physics/0408124 [physics.data-an]`.

[114] T. Chen and C. Guestrin, *XGBoost: A Scalable Tree Boosting System*, KDD '16 (2016) 785,
arXiv: `1603.02754 [cs.LG]`.

[115] J. C. Collins and D. E. Soper, *Angular distribution of dileptons in high-energy hadron collisions*, Phys. Rev. D **16** (1977) 2219.

[116] ATLAS Collaboration, *Measurement of the Drell–Yan triple-differential cross section in pp collisions at $\sqrt{s} = 8\,TeV$*, JHEP **12** (2017) 059, arXiv: `1710.05167 [hep-ex]`.

[117] ATLAS Collaboration, *Quark versus Gluon Jet Tagging Using Charged-Particle Constituent Multiplicity with the ATLAS Detector*, ATL-PHYS-PUB-2017-009, 2017, URL: `https://cds.cern.ch/record/2263679`.

[118] ATLAS Collaboration, *Measurement of the charged-particle multiplicity inside jets from $\sqrt{s} = 8\,TeV\ pp$ collisions with the ATLAS detector*, Eur. Phys. J. C **76** (2016) 322, arXiv: `1602.00988 [hep-ex]`.

[119] M. Oreglia, *A Study of the Reactions $\psi' \to \gamma\gamma\psi$*, SLAC-R-0236 (1980), URL: `www.slac.stanford.edu/cgi-wrap/getdoc/slac-r-236.pdf`.

[120] ATLAS Collaboration, *Search for Scalar Diphoton Resonances in the Mass Range 65–600 GeV with the ATLAS Detector in pp Collision Data at $\sqrt{s} = 8\,TeV$*, Phys. Rev. Lett. **113** (2014) 171801, arXiv: `1407.6583 [hep-ex]`.

[121] X. Liu and F. Petriello, *Reducing theoretical uncertainties for exclusive Higgs-boson plus one-jet production at the LHC*, Phys. Rev. D **87** (2013) 094027, arXiv: `1303.4405 [hep-ph]`.

[122] R. Boughezal, X. Liu, F. Petriello, F. J. Tackmann and J. R. Walsh, *Combining Resummed Higgs Predictions Across Jet Bins*, Phys. Rev. D **89** (2014) 074044, arXiv: `1312.4535 [hep-ph]`.

[123] J. M. Campbell and R. Ellis, *MCFM for the Tevatron and the LHC*, Nucl. Phys. B Proc. Suppl. **205-206** (2010) 10, ed. by J. Blümlein, S.-O. Moch and T. Riemann, arXiv: `1007.3492 [hep-ph]`.

[124] I. W. Stewart and F. J. Tackmann, *Theory Uncertainties for Higgs and Other Searches Using Jet Bins*, Phys. Rev. D **85** (2012) 034011, arXiv: `1107.2117 [hep-ph]`.

[125] S. Gangal and F. J. Tackmann, *Next-to-leading-order uncertainties in Higgs+2 jets from gluon fusion*, Phys. Rev. D **87** (2013) 093008, arXiv: `1302.5437 [hep-ph]`.

[126] R. Frederix, S. Frixione, E. Vryonidou and M. Wiesemann, *Heavy-quark mass effects in Higgs plus jets production*, JHEP **08** (2016) 006, arXiv: `1604.03017 [hep-ph]`.

[127] D. de Florian, G. Ferrera, M. Grazzini and D. Tommasini, *Higgs boson production at the LHC: transverse momentum resummation effects in the $H \to \gamma\gamma$, $H \to WW \to l\nu l\nu$ and $H \to ZZ \to 4l$ decay modes*, JHEP **06** (2012) 132, arXiv: `1203.6321 [hep-ph]`.

[128] M. Grazzini and H. Sargsyan, *Heavy-quark mass effects in Higgs boson production at the LHC*, JHEP **09** (2013) 129, arXiv: `1306.4581 [hep-ph]`.

[129] M. Bähr et al., *Herwig++ physics and manual*, Eur. Phys. J. C **58** (2008) 639, arXiv: `0803.0883 [hep-ph]`.

[130] J. Bellm et al., *Herwig 7.0/Herwig++ 3.0 release note*, Eur. Phys. J. C **76** (2016) 196, arXiv: 1512.01178 [hep-ph].

[131] ATLAS Collaboration, *Muon reconstruction performance of the ATLAS detector in proton–proton collision data at $\sqrt{s} = 13\,TeV$*, Eur. Phys. J. C **76** (2016) 292, arXiv: 1603.05598 [hep-ex].

[132] ATLAS Collaboration, *Performance of the ATLAS muon triggers in Run 2*, JINST **15** (2020) P09015, arXiv: 2004.13447 [hep-ex].

[133] ATLAS Collaboration, *Jet energy scale measurements and their systematic uncertainties in proton–proton collisions at $\sqrt{s} = 13\,TeV$ with the ATLAS detector*, Phys. Rev. D **96** (2017) 072002, arXiv: 1703.09665 [hep-ex].

[134] ATLAS Collaboration, *Luminosity determination in pp collisions at $\sqrt{s} = 13\,TeV$ using the ATLAS detector at the LHC*, ATLAS-CONF-2019-021, 2019, URL: https://cds.cern.ch/record/2677054.

[135] G. Avoni et al., *The new LUCID-2 detector for luminosity measurement and monitoring in ATLAS*, JINST **13** (2018) P07017.

[136] G. Cowan, K. Cranmer, E. Gross and O. Vitells, *Asymptotic formulae for likelihood-based tests of new physics*, Eur. Phys. J. C **71** (2011) 1554, [Erratum: Eur. Phys. J. C **73** (2013) 2501], arXiv: 1007.1727 [physics.data-an].

[137] Cousin, R. D., *Generalization of Chisquare Goodness-of-Fit Test for Binned Data Using Saturated Models , with Application to Histograms*, 2013, URL: https://www.semanticscholar.org/paper/Generalization-of-Chisquare-Goodness-ofFit-Test-for-Cousins/f816576fdb04547e4db2f72656136060849b3ecf.

[138] A. L. Read, *Presentation of search results: The CLs technique*, J. Phys. G **28** (2002) 2693.

[139] ATLAS Collaboration, *ATLAS Computing Acknowledgements*, ATL-SOFT-PUB-2020-001, URL: https://cds.cern.ch/record/2717821.

[140] V. Bertone, S. Carrazza and J. Rojo, *APFEL: A PDF Evolution Library with QED corrections*, Comput. Phys. Commun. **185** (2014) 1647, arXiv: 1310.1394 [hep-ph].

[141] A. Buckley et al., *LHAPDF6: parton density access in the LHC precision era*, Eur. Phys. J. C **75** (2015) 132, arXiv: 1412.7420 [hep-ph].

[142] M. Tanabashi et al. (Particle Data Group), *Review of Particle Physics*, Phys. Rev. D **98** (2018) 030001.

The ATLAS Collaboration

G. Aad[102], B. Abbott[128], D.C. Abbott[103], A. Abed Abud[36], K. Abeling[53], D.K. Abhayasinghe[94], S.H. Abidi[167], O.S. AbouZeid[40], N.L. Abraham[156], H. Abramowicz[161], H. Abreu[160], Y. Abulaiti[6], B.S. Acharya[67a,67b,n], B. Achkar[53], L. Adam[100], C. Adam Bourdarios[5], L. Adamczyk[84a], L. Adamek[167], J. Adelman[121], M. Adersberger[114], A. Adiguzel[12c], S. Adorni[54], T. Adye[143], A.A. Affolder[145], Y. Afik[160], C. Agapopoulou[65], M.N. Agaras[38], A. Aggarwal[119], C. Agheorghiesei[27c], J.A. Aguilar-Saavedra[139f,139a,ab], A. Ahmad[36], F. Ahmadov[80], W.S. Ahmed[104], X. Ai[18], G. Aielli[74a,74b], S. Akatsuka[86], M. Akbiyik[100], T.P.A. Åkesson[97], E. Akilli[54], A.V. Akimov[111], K. Al Khoury[65], G.L. Alberghi[23b,23a], J. Albert[176], M.J. Alconada Verzini[161], S. Alderweireldt[36], M. Aleksa[36], I.N. Aleksandrov[80], C. Alexa[27b], T. Alexopoulos[10], A. Alfonsi[120], F. Alfonsi[23b,23a], M. Alhroob[128], B. Ali[141], S. Ali[158], M. Aliev[166], G. Alimonti[69a], C. Allaire[36], B.M.M. Allbrooke[156], B.W. Allen[131], P.P. Allport[21], A. Aloisio[70a,70b], F. Alonso[89], C. Alpigiani[148], E. Alunno Camelia[74a,74b], M. Alvarez Estevez[99], M.G. Alviggi[70a,70b], Y. Amaral Coutinho[81b], A. Ambler[104], L. Ambroz[134], C. Amelung[36], D. Amidei[106], S.P. Amor Dos Santos[139a], S. Amoroso[46], C.S. Amrouche[54], F. An[79], C. Anastopoulos[149], N. Andari[144], T. Andeen[11], J.K. Anders[20], S.Y. Andrean[45a,45b], A. Andreazza[69a,69b], V. Andrei[61a], C.R. Anelli[176], S. Angelidakis[9], A. Angerami[39], A.V. Anisenkov[122b,122a], A. Annovi[72a], C. Antel[54], M.T. Anthony[149], E. Antipov[129], M. Antonelli[51], D.J.A. Antrim[171], F. Anulli[73a], M. Aoki[82], J.A. Aparisi Pozo[174], M.A. Aparo[156], L. Aperio Bella[46], N. Aranzabal[36], V. Araujo Ferraz[81a], R. Araujo Pereira[81b], C. Arcangeletti[51], A.T.H. Arce[49], F.A. Arduh[89], J-F. Arguin[110], S. Argyropoulos[52], J.-H. Arling[46], A.J. Armbruster[36], A. Armstrong[171], O. Arnaez[167], H. Arnold[120], Z.P. Arrubarrena Tame[114], G. Artoni[134], H. Asada[117], K. Asai[126], S. Asai[163], T. Asawatavonvanich[165], N. Asbah[59], E.M. Asimakopoulou[172], L. Asquith[156], J. Assahsah[35d], K. Assamagan[29], R. Astalos[28a], R.J. Atkin[33a], M. Atkinson[173], N.B. Atlay[19], H. Atmani[65], P.A. Atmasiddha[106], K. Augsten[141], V.A. Austrup[182], G. Avolio[36], M.K. Ayoub[15a], G. Azuelos[110,ai], D. Babal[28a], H. Bachacou[144], K. Bachas[162], F. Backman[45a,45b], P. Bagnaia[73a,73b], M. Bahmani[85], H. Bahrasemani[152], A.J. Bailey[174], V.R. Bailey[173], J.T. Baines[143], C. Bakalis[10], O.K. Baker[183], P.J. Bakker[120], E. Bakos[16], D. Bakshi Gupta[8], S. Balaji[157], R. Balasubramanian[120], E.M. Baldin[122b,122a], P. Balek[180], F. Balli[144], W.K. Balunas[134], J. Balz[100], E. Banas[85], M. Bandieramonte[138], A. Bandyopadhyay[24], Sw. Banerjee[181,i], L. Barak[161], W.M. Barbe[38], E.L. Barberio[105], D. Barberis[55b,55a], M. Barbero[102], G. Barbour[95], T. Barillari[115], M-S. Barisits[36], J. Barkeloo[131], T. Barklow[153], R. Barnea[160], B.M. Barnett[143], R.M. Barnett[18], Z. Barnovska-Blenessy[60a], A. Baroncelli[60a], G. Barone[29], A.J. Barr[134], L. Barranco Navarro[45a,45b], F. Barreiro[99], J. Barreiro Guimarães da Costa[15a], U. Barron[161], S. Barsov[137], F. Bartels[61a], R. Bartoldus[153], G. Bartolini[102], A.E. Barton[90], P. Bartos[28a], A. Basalaev[46], A. Basan[100], A. Bassalat[65,af], M.J. Basso[167], R.L. Bates[57], S. Batlamous[35e], J.R. Batley[32], B. Batool[151], M. Battaglia[145], M. Bauce[73a,73b], F. Bauer[144], P. Bauer[24], H.S. Bawa[31], A. Bayirli[12c], J.B. Beacham[49], T. Beau[135], P.H. Beauchemin[170], F. Becherer[52], P. Bechtle[24], H.C. Beck[53], H.P. Beck[20,p], K. Becker[178], C. Becot[46], A. Beddall[12d], A.J. Beddall[12a], V.A. Bednyakov[80], M. Bedognetti[120], C.P. Bee[155], T.A. Beermann[182], M. Begalli[81b], M. Begel[29], A. Behera[155], J.K. Behr[46], F. Beisiegel[24], M. Belfkir[5], A.S. Bell[95], G. Bella[161], L. Bellagamba[23b], A. Bellerive[34], P. Bellos[9], K. Beloborodov[122b,122a], K. Belotskiy[112], N.L. Belyaev[112], D. Benchekroun[35a], N. Benekos[10], Y. Benhammou[161], D.P. Benjamin[6], M. Benoit[29], J.R. Bensinger[26], S. Bentvelsen[120], L. Beresford[134], M. Beretta[51], D. Berge[19], E. Bergeaas Kuutmann[172], N. Berger[5], B. Bergmann[141], L.J. Bergsten[26], J. Beringer[18], S. Berlendis[7], G. Bernardi[135], C. Bernius[153], F.U. Bernlochner[24], T. Berry[94], P. Berta[100], A. Berthold[48], I.A. Bertram[90], O. Bessidskaia Bylund[182], N. Besson[144], A. Bethani[101], S. Bethke[115], A. Betti[42], A.J. Bevan[93], J. Beyer[115], S. Bhatta[155], D.S. Bhattacharya[177], P. Bhattarai[26], V.S. Bhopatkar[6], R. Bi[138], R.M. Bianchi[138], O. Biebel[114], D. Biedermann[19], R. Bielski[36], K. Bierwagen[100],

N.V. Biesuz[72a,72b], M. Biglietti[75a], T.R.V. Billoud[141], M. Bindi[53], A. Bingul[12d], C. Bini[73a,73b], S. Biondi[23b,23a], C.J. Birch-sykes[101], M. Birman[180], T. Bisanz[36], J.P. Biswal[3], D. Biswas[181,i], A. Bitadze[101], C. Bittrich[48], K. Bjørke[133], T. Blazek[28a], I. Bloch[46], C. Blocker[26], A. Blue[57], U. Blumenschein[93], G.J. Bobbink[120], V.S. Bobrovnikov[122b,122a], S.S. Bocchetta[97], D. Bogavac[14], A.G. Bogdanchikov[122b,122a], C. Bohm[45a], V. Boisvert[94], P. Bokan[172,53], T. Bold[84a], A.E. Bolz[61b], M. Bomben[135], M. Bona[93], J.S. Bonilla[131], M. Boonekamp[144], C.D. Booth[94], A.G. Borbély[57], H.M. Borecka-Bielska[91], L.S. Borgna[95], A. Borisov[123], G. Borissov[90], D. Bortoletto[134], D. Boscherini[23b], M. Bosman[14], J.D. Bossio Sola[104], K. Bouaouda[35a], J. Boudreau[138], E.V. Bouhova-Thacker[90], D. Boumediene[38], A. Boveia[127], J. Boyd[36], D. Boye[33c], I.R. Boyko[80], A.J. Bozson[94], J. Bracinik[21], N. Brahimi[60d], G. Brandt[182], O. Brandt[32], F. Braren[46], B. Brau[103], J.E. Brau[131], W.D. Breaden Madden[57], K. Brendlinger[46], R. Brener[160], L. Brenner[36], R. Brenner[172], S. Bressler[180], B. Brickwedde[100], D.L. Briglin[21], D. Britton[57], D. Britzger[115], I. Brock[24], R. Brock[107], G. Brooijmans[39], W.K. Brooks[146d], E. Brost[29], P.A. Bruckman de Renstrom[85], B. Brüers[46], D. Bruncko[28b], A. Bruni[23b], G. Bruni[23b], M. Bruschi[23b], N. Bruscino[73a,73b], L. Bryngemark[153], T. Buanes[17], Q. Buat[155], P. Buchholz[151], A.G. Buckley[57], I.A. Budagov[80], M.K. Bugge[133], F. Bührer[52], O. Bulekov[112], B.A. Bullard[59], T.J. Burch[121], S. Burdin[91], C.D. Burgard[120], A.M. Burger[129], B. Burghgrave[8], J.T.P. Burr[46], C.D. Burton[11], J.C. Burzynski[103], V. Büscher[100], E. Buschmann[53], P.J. Bussey[57], J.M. Butler[25], C.M. Buttar[57], J.M. Butterworth[95], P. Butti[36], W. Buttinger[143], C.J. Buxo Vazquez[107], A. Buzatu[158], A.R. Buzykaev[122b,122a], G. Cabras[23b,23a], S. Cabrera Urbán[174], D. Caforio[56], H. Cai[138], V.M.M. Cairo[153], O. Cakir[4a], N. Calace[36], P. Calafiura[18], G. Calderini[135], P. Calfayan[66], G. Callea[57], L.P. Caloba[81b], A. Caltabiano[74a,74b], S. Calvente Lopez[99], D. Calvet[38], S. Calvet[38], T.P. Calvet[102], M. Calvetti[72a,72b], R. Camacho Toro[135], S. Camarda[36], D. Camarero Munoz[99], P. Camarri[74a,74b], M.T. Camerlingo[75a,75b], D. Cameron[133], C. Camincher[36], S. Campana[36], M. Campanelli[95], A. Camplani[40], V. Canale[70a,70b], A. Canesse[104], M. Cano Bret[78], J. Cantero[129], T. Cao[161], Y. Cao[173], M.D.M. Capeans Garrido[36], M. Capua[41b,41a], R. Cardarelli[74a], F. Cardillo[174], G. Carducci[41b,41a], I. Carli[142], T. Carli[36], G. Carlino[70a], B.T. Carlson[138], E.M. Carlson[176,168a], L. Carminati[69a,69b], R.M.D. Carney[153], S. Caron[119], E. Carquin[146d], S. Carrá[46], G. Carratta[23b,23a], J.W.S. Carter[167], T.M. Carter[50], M.P. Casado[14,f], A.F. Casha[167], E.G. Castiglia[183], F.L. Castillo[174], L. Castillo Garcia[14], V. Castillo Gimenez[174], N.F. Castro[139a,139e], A. Catinaccio[36], J.R. Catmore[133], A. Cattai[36], V. Cavaliere[29], V. Cavasinni[72a,72b], E. Celebi[12b], F. Celli[134], K. Cerny[130], A.S. Cerqueira[81a], A. Cerri[156], L. Cerrito[74a,74b], F. Cerutti[18], A. Cervelli[23b,23a], S.A. Cetin[12b], Z. Chadi[35a], D. Chakraborty[121], J. Chan[181], W.S. Chan[120], W.Y. Chan[91], J.D. Chapman[32], B. Chargeishvili[159b], D.G. Charlton[21], T.P. Charman[93], M. Chatterjee[20], C.C. Chau[34], S. Che[127], S. Chekanov[6], S.V. Chekulaev[168a], G.A. Chelkov[80,ad], B. Chen[79], C. Chen[60a], C.H. Chen[79], H. Chen[15c], H. Chen[29], J. Chen[60a], J. Chen[39], J. Chen[26], S. Chen[136], S.J. Chen[15c], X. Chen[15b], Y. Chen[60a], Y-H. Chen[46], H.C. Cheng[63a], H.J. Cheng[15a], A. Cheplakov[80], E. Cheremushkina[123], R. Cherkaoui El Moursli[35e], E. Cheu[7], K. Cheung[64], T.J.A. Chevalérias[144], L. Chevalier[144], V. Chiarella[51], G. Chiarelli[72a], G. Chiodini[68a], A.S. Chisholm[21], A. Chitan[27b], I. Chiu[163], Y.H. Chiu[176], M.V. Chizhov[80], K. Choi[11], A.R. Chomont[73a,73b], Y.S. Chow[120], L.D. Christopher[33e], M.C. Chu[63a], X. Chu[15a,15d], J. Chudoba[140], J.J. Chwastowski[85], L. Chytka[130], D. Cieri[115], K.M. Ciesla[85], V. Cindro[92], I.A. Cioară[27b], A. Ciocio[18], F. Cirotto[70a,70b], Z.H. Citron[180,j], M. Citterio[69a], D.A. Ciubotaru[27b], B.M. Ciungu[167], A. Clark[54], P.J. Clark[50], S.E. Clawson[101], C. Clement[45a,45b], Y. Coadou[102], M. Cobal[67a,67c], A. Coccaro[55b], J. Cochran[79], R. Coelho Lopes De Sa[103], H. Cohen[161], A.E.C. Coimbra[36], B. Cole[39], A.P. Colijn[120], J. Collot[58], P. Conde Muiño[139a,139h], S.H. Connell[33c], I.A. Connelly[57], S. Constantinescu[27b], F. Conventi[70a,aj], A.M. Cooper-Sarkar[134], F. Cormier[175], K.J.R. Cormier[167], L.D. Corpe[95], M. Corradi[73a,73b], E.E. Corrigan[97], F. Corriveau[104,z], M.J. Costa[174], F. Costanza[5], D. Costanzo[149], G. Cowan[94], J.W. Cowley[32], J. Crane[101], K. Cranmer[125], R.A. Creager[136], S. Crépé-Renaudin[58], F. Crescioli[135], M. Cristinziani[24], V. Croft[170], G. Crosetti[41b,41a], A. Cueto[5], T. Cuhadar Donszelmann[171],

H. Cui[15a,15d], A.R. Cukierman[153], W.R. Cunningham[57], S. Czekierda[85], P. Czodrowski[36],
M.M. Czurylo[61b], M.J. Da Cunha Sargedas De Sousa[60b], J.V. Da Fonseca Pinto[81b], C. Da Via[101],
W. Dabrowski[84a], F. Dachs[36], T. Dado[47], S. Dahbi[33e], T. Dai[106], C. Dallapiccola[103], M. Dam[40],
G. D'amen[29], V. D'Amico[75a,75b], J. Damp[100], J.R. Dandoy[136], M.F. Daneri[30], M. Danninger[152], V. Dao[36],
G. Darbo[55b], O. Dartsi[5], A. Dattagupta[131], T. Daubney[46], S. D'Auria[69a,69b], C. David[168b], T. Davidek[142],
D.R. Davis[49], I. Dawson[149], K. De[8], R. De Asmundis[70a], M. De Beurs[120], S. De Castro[23b,23a],
N. De Groot[119], P. de Jong[120], H. De la Torre[107], A. De Maria[15c], D. De Pedis[73a], A. De Salvo[73a],
U. De Sanctis[74a,74b], M. De Santis[74a,74b], A. De Santo[156], J.B. De Vivie De Regie[65], D.V. Dedovich[80],
A.M. Deiana[42], J. Del Peso[99], Y. Delabat Diaz[46], D. Delgove[65], F. Deliot[144], C.M. Delitzsch[7],
M. Della Pietra[70a,70b], D. Della Volpe[54], A. Dell'Acqua[36], L. Dell'Asta[74a,74b], M. Delmastro[5],
C. Delporte[65], P.A. Delsart[58], S. Demers[183], M. Demichev[80], G. Demontigny[110], S.P. Denisov[123],
L. D'Eramo[121], D. Derendarz[85], J.E. Derkaoui[35d], F. Derue[135], P. Dervan[91], K. Desch[24], K. Dette[167],
C. Deutsch[24], M.R. Devesa[30], P.O. Deviveiros[36], F.A. Di Bello[73a,73b], A. Di Ciaccio[74a,74b], L. Di Ciaccio[5],
W.K. Di Clemente[136], C. Di Donato[70a,70b], A. Di Girolamo[36], G. Di Gregorio[72a,72b], B. Di Micco[75a,75b],
R. Di Nardo[75a,75b], K.F. Di Petrillo[59], R. Di Sipio[167], C. Diaconu[102], F.A. Dias[120], T. Dias Do Vale[139a],
M.A. Diaz[146a], F.G. Diaz Capriles[24], J. Dickinson[18], M. Didenko[166], E.B. Diehl[106], J. Dietrich[19],
S. Díez Cornell[46], C. Diez Pardos[151], A. Dimitrievska[18], W. Ding[15b], J. Dingfelder[24], S.J. Dittmeier[61b],
F. Dittus[36], F. Djama[102], T. Djobava[159b], J.I. Djuvsland[17], M.A.B. Do Vale[147], M. Dobre[27b],
D. Dodsworth[26], C. Doglioni[97], J. Dolejsi[142], Z. Dolezal[142], M. Donadelli[81c], B. Dong[60c], J. Donini[38],
A. D'onofrio[15c], M. D'Onofrio[91], J. Dopke[143], A. Doria[70a], M.T. Dova[89], A.T. Doyle[57], E. Drechsler[152],
E. Dreyer[152], T. Dreyer[53], A.S. Drobac[170], D. Du[60b], T.A. du Pree[120], Y. Duan[60d], F. Dubinin[111],
M. Dubovsky[28a], A. Dubreuil[54], E. Duchovni[180], G. Duckeck[114], O.A. Ducu[36], D. Duda[115], A. Dudarev[36],
A.C. Dudder[100], E.M. Duffield[18], M. D'uffizi[101], L. Duflot[65], M. Dührssen[36], C. Dülsen[182],
M. Dumancic[180], A.E. Dumitriu[27b], M. Dunford[61a], S. Dungs[47], A. Duperrin[102], H. Duran Yildiz[4a],
M. Düren[56], A. Durglishvili[159b], D. Duschinger[48], B. Dutta[46], D. Duvnjak[1], G.I. Dyckes[136], M. Dyndal[36],
S. Dysch[101], B.S. Dziedzic[85], M.G. Eggleston[49], T. Eifert[8], G. Eigen[17], K. Einsweiler[18], T. Ekelof[172],
H. El Jarrari[35e], V. Ellajosyula[172], M. Ellert[172], F. Ellinghaus[182], A.A. Elliot[93], N. Ellis[36], J. Elmsheuser[29],
M. Elsing[36], D. Emeliyanov[143], A. Emerman[39], Y. Enari[163], M.B. Epland[49], J. Erdmann[47], A. Ereditato[20],
P.A. Erland[85], M. Errenst[182], M. Escalier[65], C. Escobar[174], O. Estrada Pastor[174], E. Etzion[161],
G.E. Evans[139a,139b], H. Evans[66], M.O. Evans[156], A. Ezhilov[137], F. Fabbri[57], L. Fabbri[23b,23a], V. Fabiani[119],
G. Facini[178], R.M. Fakhrutdinov[123], S. Falciano[73a], P.J. Falke[24], S. Falke[36], J. Faltova[142], Y. Fang[15a],
Y. Fang[15a], G. Fanourakis[44], M. Fanti[69a,69b], M. Faraj[67a,67c], A. Farbin[8], A. Farilla[75a], E.M. Farina[71a,71b],
T. Farooque[107], S.M. Farrington[50], P. Farthouat[36], F. Fassi[35e], P. Fassnacht[36], D. Fassouliotis[9],
M. Faucci Giannelli[50], W.J. Fawcett[32], L. Fayard[65], O.L. Fedin[137,o], W. Fedorko[175], A. Fehr[20],
M. Feickert[173], L. Feligioni[102], A. Fell[149], C. Feng[60b], M. Feng[49], M.J. Fenton[171], A.B. Fenyuk[123],
S.W. Ferguson[43], J. Ferrando[46], A. Ferrari[172], P. Ferrari[120], R. Ferrari[71a], D.E. Ferreira de Lima[61b],
A. Ferrer[174], D. Ferrere[54], C. Ferretti[106], F. Fiedler[100], A. Filipčič[92], F. Filthaut[119], K.D. Finelli[25],
M.C.N. Fiolhais[139a,139c,a], L. Fiorini[174], F. Fischer[114], J. Fischer[100], W.C. Fisher[107], T. Fitschen[21],
I. Fleck[151], P. Fleischmann[106], T. Flick[182], B.M. Flierl[114], L. Flores[136], L.R. Flores Castillo[63a],
F.M. Follega[76a,76b], N. Fomin[17], J.H. Foo[167], G.T. Forcolin[76a,76b], B.C. Forland[66], A. Formica[144],
F.A. Förster[14], A.C. Forti[101], E. Fortin[102], M.G. Foti[134], D. Fournier[65], H. Fox[90], P. Francavilla[72a,72b],
S. Francescato[73a,73b], M. Franchini[23b,23a], S. Franchino[61a], D. Francis[36], L. Franco[5], L. Franconi[20],
M. Franklin[59], G. Frattari[73a,73b], A.N. Fray[93], P.M. Freeman[21], B. Freund[110], W.S. Freund[81b],
E.M. Freundlich[47], D.C. Frizzell[128], D. Froidevaux[36], J.A. Frost[134], M. Fujimoto[126], C. Fukunaga[164],
E. Fullana Torregrosa[174], T. Fusayasu[116], J. Fuster[174], A. Gabrielli[23b,23a], A. Gabrielli[36], S. Gadatsch[54],
P. Gadow[115], G. Gagliardi[55b,55a], L.G. Gagnon[110], G.E. Gallardo[134], E.J. Gallas[134], B.J. Gallop[143],
R. Gamboa Goni[93], K.K. Gan[127], S. Ganguly[180], J. Gao[60a], Y. Gao[50], Y.S. Gao[31,l], F.M. Garay Walls[146a],

C. García[174], J.E. García Navarro[174], J.A. García Pascual[15a], C. Garcia-Argos[52], M. Garcia-Sciveres[18],
R.W. Gardner[37], N. Garelli[153], S. Gargiulo[52], C.A. Garner[167], V. Garonne[133], S.J. Gasiorowski[148],
P. Gaspar[81b], A. Gaudiello[55b,55a], G. Gaudio[71a], P. Gauzzi[73a,73b], I.L. Gavrilenko[111], A. Gavrilyuk[124],
C. Gay[175], G. Gaycken[46], E.N. Gazis[10], A.A. Geanta[27b], C.M. Gee[145], C.N.P. Gee[143], J. Geisen[97],
M. Geisen[100], C. Gemme[55b], M.H. Genest[58], C. Geng[106], S. Gentile[73a,73b], S. George[94], T. Geralis[44],
L.O. Gerlach[53], P. Gessinger-Befurt[100], G. Gessner[47], S. Ghasemi[151], M. Ghasemi Bostanabad[176],
M. Ghneimat[151], A. Ghosh[65], A. Ghosh[78], B. Giacobbe[23b], S. Giagu[73a,73b], N. Giangiacomi[23b,23a],
P. Giannetti[72a], A. Giannini[70a,70b], G. Giannini[14], S.M. Gibson[94], M. Gignac[145], D.T. Gil[84b], B.J. Gilbert[39],
D. Gillberg[34], G. Gilles[182], N.E.K. Gillwald[46], D.M. Gingrich[3,ai], M.P. Giordani[67a,67c], P.F. Giraud[144],
G. Giugliarelli[67a,67c], D. Giugni[69a], F. Giuli[74a,74b], S. Gkaitatzis[162], I. Gkialas[9,g], E.L. Gkougkousis[14],
P. Gkountoumis[10], L.K. Gladilin[113], C. Glasman[99], J. Glatzer[14], P.C.F. Glaysher[46], A. Glazov[46],
G.R. Gledhill[131], I. Gnesi[41b,b], M. Goblirsch-Kolb[26], D. Godin[110], S. Goldfarb[105], T. Golling[54],
D. Golubkov[123], A. Gomes[139a,139b], R. Goncalves Gama[53], R. Gonçalo[139a,139c], G. Gonella[131],
L. Gonella[21], A. Gongadze[80], F. Gonnella[21], J.L. Gonski[39], S. González de la Hoz[174],
S. Gonzalez Fernandez[14], R. Gonzalez Lopez[91], C. Gonzalez Renteria[18], R. Gonzalez Suarez[172],
S. Gonzalez-Sevilla[54], G.R. Gonzalvo Rodriguez[174], L. Goossens[36], N.A. Gorasia[21], P.A. Gorbounov[124],
H.A. Gordon[29], B. Gorini[36], E. Gorini[68a,68b], A. Gorišek[92], A.T. Goshaw[49], M.I. Gostkin[80],
C.A. Gottardo[119], M. Gouighri[35b], A.G. Goussiou[148], N. Govender[33c], C. Goy[5], I. Grabowska-Bold[84a],
E.C. Graham[91], J. Gramling[171], E. Gramstad[133], S. Grancagnolo[19], M. Grandi[156], V. Gratchev[137],
P.M. Gravila[27f], F.G. Gravili[68a,68b], C. Gray[57], H.M. Gray[18], C. Grefe[24], K. Gregersen[97], I.M. Gregor[46],
P. Grenier[153], K. Grevtsov[46], C. Grieco[14], N.A. Grieser[128], A.A. Grillo[145], K. Grimm[31,k], S. Grinstein[14,v],
J.-F. Grivaz[65], S. Groh[100], E. Gross[180], J. Grosse-Knetter[53], Z.J. Grout[95], C. Grud[106], A. Grummer[118],
J.C. Grundy[134], L. Guan[106], W. Guan[181], C. Gubbels[175], J. Guenther[77], A. Guerguichon[65],
J.G.R. Guerrero Rojas[174], F. Guescini[115], D. Guest[77], R. Gugel[100], A. Guida[46], T. Guillemin[5],
S. Guindon[36], J. Guo[60c], W. Guo[106], Y. Guo[60a], Z. Guo[102], R. Gupta[46], S. Gurbuz[12c], G. Gustavino[128],
M. Guth[52], P. Gutierrez[128], C. Gutschow[95], C. Guyot[144], C. Gwenlan[134], C.B. Gwilliam[91],
E.S. Haaland[133], A. Haas[125], C. Haber[18], H.K. Hadavand[8], A. Hadef[60a], M. Haleem[177], J. Haley[129],
J.J. Hall[149], G. Halladjian[107], G.D. Hallewell[102], K. Hamano[176], H. Hamdaoui[35e], M. Hamer[24],
G.N. Hamity[50], K. Han[60a], L. Han[15c], L. Han[60a], S. Han[18], Y.F. Han[167], K. Hanagaki[82,t], M. Hance[145],
D.M. Handl[114], M.D. Hank[37], R. Hankache[135], E. Hansen[97], J.B. Hansen[40], J.D. Hansen[40],
M.C. Hansen[24], P.H. Hansen[40], E.C. Hanson[101], K. Hara[169], T. Harenberg[182], S. Harkusha[108],
P.F. Harrison[178], N.M. Hartman[153], N.M. Hartmann[114], Y. Hasegawa[150], A. Hasib[50], S. Hassani[144],
S. Haug[20], R. Hauser[107], M. Havranek[141], C.M. Hawkes[21], R.J. Hawkings[36], S. Hayashida[117],
D. Hayden[107], C. Hayes[106], R.L. Hayes[175], C.P. Hays[134], J.M. Hays[93], H.S. Hayward[91], S.J. Haywood[143],
F. He[60a], Y. He[165], M.P. Heath[50], V. Hedberg[97], A.L. Heggelund[133], C. Heidegger[52], K.K. Heidegger[52],
W.D. Heidorn[79], J. Heilman[34], S. Heim[46], T. Heim[18], B. Heinemann[46,ag], J.G. Heinlein[136],
J.J. Heinrich[131], L. Heinrich[36], J. Hejbal[140], L. Helary[46], A. Held[125], S. Hellesund[133], C.M. Helling[145],
S. Hellman[45a,45b], C. Helsens[36], R.C.W. Henderson[90], L. Henkelmann[32], A.M. Henriques Correia[36],
H. Herde[26], Y. Hernández Jiménez[33e], H. Herr[100], M.G. Herrmann[114], T. Herrmann[48], G. Herten[52],
R. Hertenberger[114], L. Hervas[36], T.C. Herwig[136], G.G. Hesketh[95], N.P. Hessey[168a], H. Hibi[83],
S. Higashino[82], E. Higón-Rodriguez[174], K. Hildebrand[37], J.C. Hill[32], K.K. Hill[29], K.H. Hiller[46],
S.J. Hillier[21], M. Hils[48], I. Hinchliffe[18], F. Hinterkeuser[24], M. Hirose[132], S. Hirose[169], D. Hirschbuehl[182],
B. Hiti[92], O. Hladik[140], J. Hobbs[155], R. Hobincu[27e], N. Hod[180], M.C. Hodgkinson[149], A. Hoecker[36],
D. Hohn[52], D. Hohov[65], T. Holm[24], T.R. Holmes[37], M. Holzbock[115], L.B.A.H. Hommels[32], T.M. Hong[138],
J.C. Honig[52], A. Hönle[115], B.H. Hooberman[173], W.H. Hopkins[6], Y. Horii[117], P. Horn[48], L.A. Horyn[37],
S. Hou[158], A. Hoummada[35a], J. Howarth[57], J. Hoya[89], M. Hrabovsky[130], J. Hrivnac[65], A. Hrynevich[109],
T. Hryn'ova[5], P.J. Hsu[64], S.-C. Hsu[148], Q. Hu[29], S. Hu[60c], Y.F. Hu[15a,15d,ak], D.P. Huang[95], X. Huang[15c],

31

Y. Huang[60a], Y. Huang[15a], Z. Hubacek[141], F. Hubaut[102], M. Huebner[24], F. Huegging[24], T.B. Huffman[134], M. Huhtinen[36], R. Hulsken[58], R.F.H. Hunter[34], N. Huseynov[80,aa], J. Huston[107], J. Huth[59], R. Hyneman[153], S. Hyrych[28a], G. Iacobucci[54], G. Iakovidis[29], I. Ibragimov[151], L. Iconomidou-Fayard[65], P. Iengo[36], R. Ignazzi[40], R. Iguchi[163], T. Iizawa[54], Y. Ikegami[82], M. Ikeno[82], N. Ilic[119,167,z], F. Iltzsche[48], H. Imam[35a], G. Introzzi[71a,71b], M. Iodice[75a], K. Iordanidou[168a], V. Ippolito[73a,73b], M.F. Isacson[172], M. Ishino[163], W. Islam[129], C. Issever[19,46], S. Istin[160], J.M. Iturbe Ponce[63a], R. Iuppa[76a,76b], A. Ivina[180], J.M. Izen[43], V. Izzo[70a], P. Jacka[140], P. Jackson[1], R.M. Jacobs[46], B.P. Jaeger[152], V. Jain[2], G. Jäkel[182], K.B. Jakobi[100], K. Jakobs[52], T. Jakoubek[180], J. Jamieson[57], K.W. Janas[84a], R. Jansky[54], M. Janus[53], P.A. Janus[84a], G. Jarlskog[97], A.E. Jaspan[91], N. Javadov[80,aa], T. Javůrek[36], M. Javurkova[103], F. Jeanneau[144], L. Jeanty[131], J. Jejelava[159a], P. Jenni[52,c], N. Jeong[46], S. Jézéquel[5], J. Jia[155], Z. Jia[15c], H. Jiang[79], Y. Jiang[60a], Z. Jiang[153], S. Jiggins[52], F.A. Jimenez Morales[38], J. Jimenez Pena[115], S. Jin[15c], A. Jinaru[27b], O. Jinnouchi[165], H. Jivan[33e], P. Johansson[149], K.A. Johns[7], C.A. Johnson[66], E. Jones[178], R.W.L. Jones[90], S.D. Jones[156], T.J. Jones[91], J. Jongmanns[61a], J. Jovicevic[36], X. Ju[18], J.J. Junggeburth[115], A. Juste Rozas[14,v], A. Kaczmarska[85], M. Kado[73a,73b], H. Kagan[127], M. Kagan[153], A. Kahn[39], C. Kahra[100], T. Kaji[179], E. Kajomovitz[160], C.W. Kalderon[29], A. Kaluza[100], A. Kamenshchikov[123], M. Kaneda[163], N.J. Kang[145], S. Kang[79], Y. Kano[117], J. Kanzaki[82], L.S. Kaplan[181], D. Kar[33e], K. Karava[134], M.J. Kareem[168b], I. Karkanias[162], S.N. Karpov[80], Z.M. Karpova[80], V. Kartvelishvili[90], A.N. Karyukhin[123], E. Kasimi[162], A. Kastanas[45a,45b], C. Kato[60d], J. Katzy[46], K. Kawade[150], K. Kawagoe[88], T. Kawaguchi[117], T. Kawamoto[144], G. Kawamura[53], E.F. Kay[176], S. Kazakos[14], V.F. Kazanin[122b,122a], J.M. Keaveney[33a], R. Keeler[176], J.S. Keller[34], E. Kellermann[97], D. Kelsey[156], J.J. Kempster[21], J. Kendrick[21], K.E. Kennedy[39], O. Kepka[140], S. Kersten[182], B.P. Kerševan[92], S. Ketabchi Haghighat[167], F. Khalil-Zada[13], M. Khandoga[144], A. Khanov[129], A.G. Kharlamov[122b,122a], T. Kharlamova[122b,122a], E.E. Khoda[175], A. Khodinov[166], T.J. Khoo[77], G. Khoriauli[177], E. Khramov[80], J. Khubua[159b], S. Kido[83], M. Kiehn[36], E. Kim[165], Y.K. Kim[37], N. Kimura[95], A. Kirchhoff[53], D. Kirchmeier[48], J. Kirk[143], A.E. Kiryunin[115], T. Kishimoto[163], D.P. Kisliuk[167], V. Kitali[46], C. Kitsaki[10], O. Kivernyk[24], T. Klapdor-Kleingrothaus[52], M. Klassen[61a], C. Klein[34], M.H. Klein[106], M. Klein[91], U. Klein[91], K. Kleinknecht[100], P. Klimek[36], A. Klimentov[29], T. Klingl[24], T. Klioutchnikova[36], F.F. Klitzner[114], P. Kluit[120], S. Kluth[115], E. Kneringer[77], E.B.F.G. Knoops[102], A. Knue[52], D. Kobayashi[88], M. Kobel[48], M. Kocian[153], T. Kodama[163], P. Kodys[142], D.M. Koeck[156], P.T. Koenig[24], T. Koffas[34], N.M. Köhler[36], M. Kolb[144], I. Koletsou[5], T. Komarek[130], T. Kondo[82], K. Köneke[52], A.X.Y. Kong[1], A.C. König[119], T. Kono[126], V. Konstantinides[95], N. Konstantinidis[95], B. Konya[97], R. Kopeliansky[66], S. Koperny[84a], K. Korcyl[85], K. Kordas[162], G. Koren[161], A. Korn[95], I. Korolkov[14], E.V. Korolkova[149], N. Korotkova[113], O. Kortner[115], S. Kortner[115], V.V. Kostyukhin[149,166], A. Kotsokechagia[65], A. Kotwal[49], A. Koulouris[10], A. Kourkoumeli-Charalampidi[71a,71b], C. Kourkoumelis[9], E. Kourlitis[6], V. Kouskoura[29], R. Kowalewski[176], W. Kozanecki[101], A.S. Kozhin[123], V.A. Kramarenko[113], G. Kramberger[92], D. Krasnopevtsev[60a], M.W. Krasny[135], A. Krasznahorkay[36], D. Krauss[115], J.A. Kremer[100], J. Kretzschmar[91], P. Krieger[167], F. Krieter[114], S. Krishnamurthy[103], A. Krishnan[61b], M. Krivos[142], K. Krizka[18], K. Kroeninger[47], H. Kroha[115], J. Kroll[140], J. Kroll[136], K.S. Krowpman[107], U. Kruchonak[80], H. Krüger[24], N. Krumnack[79], M.C. Kruse[49], J.A. Krzysiak[85], A. Kubota[165], O. Kuchinskaia[166], S. Kuday[4b], D. Kuechler[46], J.T. Kuechler[46], S. Kuehn[36], T. Kuhl[46], V. Kukhtin[80], Y. Kulchitsky[108,ac], S. Kuleshov[146b], Y.P. Kulinich[173], M. Kuna[58], A. Kupco[140], T. Kupfer[47], O. Kuprash[52], H. Kurashige[83], L.L. Kurchaninov[168a], Y.A. Kurochkin[108], A. Kurova[112], M.G. Kurth[15a,15d], E.S. Kuwertz[36], M. Kuze[165], A.K. Kvam[148], J. Kvita[130], T. Kwan[104], F. La Ruffa[41b,41a], C. Lacasta[174], F. Lacava[73a,73b], D.P.J. Lack[101], H. Lacker[19], D. Lacour[135], E. Ladygin[80], R. Lafaye[5], B. Laforge[135], T. Lagouri[146c], S. Lai[53], I.K. Lakomiec[84a], J.E. Lambert[128], S. Lammers[66], W. Lampl[7], C. Lampoudis[162], E. Lançon[29], U. Landgraf[52], M.P.J. Landon[93], V.S. Lang[52], J.C. Lange[53], R.J. Langenberg[103], A.J. Lankford[171], F. Lanni[29], K. Lantzsch[24], A. Lanza[71a], A. Lapertosa[55b,55a], J.F. Laporte[144], T. Lari[69a],

F. Lasagni Manghi[23b,23a], M. Lassnig[36], V. Latonova[140], T.S. Lau[63a], A. Laudrain[100], A. Laurier[34],
M. Lavorgna[70a,70b], S.D. Lawlor[94], M. Lazzaroni[69a,69b], B. Le[101], E. Le Guirriec[102], A. Lebedev[79],
M. LeBlanc[7], T. LeCompte[6], F. Ledroit-Guillon[58], A.C.A. Lee[95], C.A. Lee[29], G.R. Lee[17], L. Lee[59],
S.C. Lee[158], S. Lee[79], B. Lefebvre[168a], H.P. Lefebvre[94], M. Lefebvre[176], C. Leggett[18], K. Lehmann[152],
N. Lehmann[20], G. Lehmann Miotto[36], W.A. Leight[46], A. Leisos[162,u], M.A.L. Leite[81c], C.E. Leitgeb[114],
R. Leitner[142], K.J.C. Leney[42], T. Lenz[24], S. Leone[72a], C. Leonidopoulos[50], A. Leopold[135], C. Leroy[110],
R. Les[107], C.G. Lester[32], M. Levchenko[137], J. Levêque[5], D. Levin[106], L.J. Levinson[180], D.J. Lewis[21],
B. Li[15b], B. Li[106], C-Q. Li[60c,60d], F. Li[60c], H. Li[60a], H. Li[60b], J. Li[60c], K. Li[148], L. Li[60c], M. Li[15a,15d],
Q.Y. Li[60a], S. Li[60d,60c], X. Li[46], Y. Li[46], Z. Li[60b], Z. Li[134], Z. Li[104], Z. Li[91], Z. Liang[15a], M. Liberatore[46],
B. Liberti[74a], K. Lie[63c], S. Lim[29], C.Y. Lin[32], K. Lin[107], R.A. Linck[66], R.E. Lindley[7], J.H. Lindon[21],
A. Linss[46], A.L. Lionti[54], E. Lipeles[136], A. Lipniacka[17], T.M. Liss[173,ah], A. Lister[175], J.D. Little[8], B. Liu[79],
B.X. Liu[152], H.B. Liu[29], J.B. Liu[60a], J.K.K. Liu[37], K. Liu[60d], M. Liu[60a], M.Y. Liu[60a], P. Liu[15a], X. Liu[60a],
Y. Liu[46], Y. Liu[15a,15d], Y.L. Liu[106], Y.W. Liu[60a], M. Livan[71a,71b], A. Lleres[58], J. Llorente Merino[152],
S.L. Lloyd[93], C.Y. Lo[63b], E.M. Lobodzinska[46], P. Loch[7], S. Loffredo[74a,74b], T. Lohse[19], K. Lohwasser[149],
M. Lokajicek[140], J.D. Long[173], R.E. Long[90], I. Longarini[73a,73b], L. Longo[36], K.A. Looper[127],
I. Lopez Paz[101], A. Lopez Solis[149], J. Lorenz[114], N. Lorenzo Martinez[5], A.M. Lory[114], P.J. Lösel[114],
A. Lösle[52], X. Lou[45a,45b], X. Lou[15a], A. Lounis[65], J. Love[6], P.A. Love[90], J.J. Lozano Bahilo[174], M. Lu[60a],
Y.J. Lu[64], H.J. Lubatti[148], C. Luci[73a,73b], F.L. Lucio Alves[15c], A. Lucotte[58], F. Luehring[66], I. Luise[155],
L. Luminari[73a], B. Lund-Jensen[154], N.A. Luongo[131], M.S. Lutz[161], D. Lynn[29], H. Lyons[91], R. Lysak[140],
E. Lytken[97], F. Lyu[15a], V. Lyubushkin[80], T. Lyubushkina[80], H. Ma[29], L.L. Ma[60b], Y. Ma[95],
D.M. Mac Donell[176], G. Maccarrone[51], C.M. Macdonald[149], J.C. MacDonald[149], J. Machado Miguens[136],
D. Madaffari[174], R. Madar[38], W.F. Mader[48], M. Madugoda Ralalage Don[129], N. Madysa[48], J. Maeda[83],
T. Maeno[29], M. Maerker[48], V. Magerl[52], N. Magini[79], J. Magro[67a,67c,q], D.J. Mahon[39], C. Maidantchik[81b],
T. Maier[114], A. Maio[139a,139b,139d], K. Maj[84a], O. Majersky[28a], S. Majewski[131], Y. Makida[82], N. Makovec[65],
B. Malaescu[135], Pa. Malecki[85], V.P. Maleev[137], F. Malek[58], D. Malito[41b,41a], U. Mallik[78], C. Malone[32],
S. Maltezos[10], S. Malyukov[80], J. Mamuzic[174], G. Mancini[51], J.P. Mandalia[93], I. Mandić[92],
L. Manhaes de Andrade Filho[81a], I.M. Maniatis[162], J. Manjarres Ramos[48], K.H. Mankinen[97], A. Mann[114],
A. Manousos[77], B. Mansoulie[144], I. Manthos[162], S. Manzoni[120], A. Marantis[162], G. Marceca[30],
L. Marchese[134], G. Marchiori[135], M. Marcisovsky[140], L. Marcoccia[74a,74b], C. Marcon[97], M. Marjanovic[128],
Z. Marshall[18], M.U.F. Martensson[172], S. Marti-Garcia[174], C.B. Martin[127], T.A. Martin[178], V.J. Martin[50],
B. Martin dit Latour[17], L. Martinelli[75a,75b], M. Martinez[14,v], P. Martinez Agullo[174],
V.I. Martinez Outschoorn[103], S. Martin-Haugh[143], V.S. Martoiu[27b], A.C. Martyniuk[95], A. Marzin[36],
S.R. Maschek[115], L. Masetti[100], T. Mashimo[163], R. Mashinistov[111], J. Masik[101], A.L. Maslennikov[122b,122a],
L. Massa[23b,23a], P. Massarotti[70a,70b], P. Mastrandrea[72a,72b], A. Mastroberardino[41b,41a], T. Masubuchi[163],
D. Matakias[29], A. Matic[114], N. Matsuzawa[163], P. Mättig[24], J. Maurer[27b], B. Maček[92],
D.A. Maximov[122b,122a], R. Mazini[158], I. Maznas[162], S.M. Mazza[145], J.P. Mc Gowan[104], S.P. Mc Kee[106],
T.G. McCarthy[115], W.P. McCormack[18], E.F. McDonald[105], A.E. McDougall[120], J.A. Mcfayden[18],
G. Mchedlidze[159b], M.A. McKay[42], K.D. McLean[176], S.J. McMahon[143], P.C. McNamara[105],
C.J. McNicol[178], R.A. McPherson[176,z], J.E. Mdhluli[33e], Z.A. Meadows[103], S. Meehan[36], T. Megy[38],
S. Mehlhase[114], A. Mehta[91], B. Meirose[43], D. Melini[160], B.R. Mellado Garcia[33e], J.D. Mellenthin[53],
M. Melo[28a], F. Meloni[46], A. Melzer[24], E.D. Mendes Gouveia[139a,139e], A.M. Mendes Jacques Da Costa[21],
H.Y. Meng[167], L. Meng[36], X.T. Meng[106], S. Menke[115], E. Meoni[41b,41a], S. Mergelmeyer[19],
S.A.M. Merkt[138], C. Merlassino[134], P. Mermod[54], L. Merola[70a,70b], C. Meroni[69a], G. Merz[106],
O. Meshkov[113,111], J.K.R. Meshreki[151], J. Metcalfe[6], A.S. Mete[6], C. Meyer[66], J-P. Meyer[144],
M. Michetti[19], R.P. Middleton[143], L. Mijović[50], G. Mikenberg[180], M. Mikestikova[140], M. Mikuž[92],
H. Mildner[149], A. Milic[167], C.D. Milke[42], D.W. Miller[37], L.S. Miller[34], A. Milov[180], D.A. Milstead[45a,45b],
R.A. Mina[153], A.A. Minaenko[123], I.A. Minashvili[159b], L. Mince[57], A.I. Mincer[125], B. Mindur[84a],

M. Mineev[80], Y. Minegishi[163], Y. Mino[86], L.M. Mir[14], M. Mironova[134], K.P. Mistry[136], T. Mitani[179],
J. Mitrevski[114], V.A. Mitsou[174], M. Mittal[60c], O. Miu[167], A. Miucci[20], P.S. Miyagawa[93], A. Mizukami[82],
J.U. Mjörnmark[97], T. Mkrtchyan[61a], M. Mlynarikova[121], T. Moa[45a,45b], S. Mobius[53], K. Mochizuki[110],
P. Moder[46], P. Mogg[114], S. Mohapatra[39], R. Moles-Valls[24], K. Mönig[46], E. Monnier[102], A. Montalbano[152],
J. Montejo Berlingen[36], M. Montella[95], F. Monticelli[89], S. Monzani[69a], N. Morange[65],
A.L. Moreira De Carvalho[139a], D. Moreno[22a], M. Moreno Llácer[174], C. Moreno Martinez[14],
P. Morettini[55b], M. Morgenstern[160], S. Morgenstern[48], D. Mori[152], M. Morii[59], M. Morinaga[179],
V. Morisbak[133], A.K. Morley[36], G. Mornacchi[36], A.P. Morris[95], L. Morvaj[36], P. Moschovakos[36],
B. Moser[120], M. Mosidze[159b], T. Moskalets[144], P. Moskvitina[119], J. Moss[31,m], E.J.W. Moyse[103],
S. Muanza[102], J. Mueller[138], R.S.P. Mueller[114], D. Muenstermann[90], G.A. Mullier[97], D.P. Mungo[69a,69b],
J.L. Munoz Martinez[14], F.J. Munoz Sanchez[101], P. Murin[28b], W.J. Murray[178,143], A. Murrone[69a,69b],
J.M. Muse[128], M. Muškinja[18], C. Mwewa[33a], A.G. Myagkov[123,ad], A.A. Myers[138], G. Myers[66],
J. Myers[131], M. Myska[141], B.P. Nachman[18], O. Nackenhorst[47], A.Nag Nag[48], K. Nagai[134], K. Nagano[82],
Y. Nagasaka[62], J.L. Nagle[29], E. Nagy[102], A.M. Nairz[36], Y. Nakahama[117], K. Nakamura[82], T. Nakamura[163],
H. Nanjo[132], F. Napolitano[61a], R.F. Naranjo Garcia[46], R. Narayan[42], I. Naryshkin[137], M. Naseri[34],
T. Naumann[46], G. Navarro[22a], P.Y. Nechaeva[111], F. Nechansky[46], T.J. Neep[21], A. Negri[71a,71b],
M. Negrini[23b], C. Nellist[119], C. Nelson[104], M.E. Nelson[45a,45b], S. Nemecek[140], M. Nessi[36,e],
M.S. Neubauer[173], F. Neuhaus[100], M. Neumann[182], R. Newhouse[175], P.R. Newman[21], C.W. Ng[138],
Y.S. Ng[19], Y.W.Y. Ng[171], B. Ngair[35e], H.D.N. Nguyen[102], T. Nguyen Manh[110], E. Nibigira[38],
R.B. Nickerson[134], R. Nicolaidou[144], D.S. Nielsen[40], J. Nielsen[145], M. Niemeyer[53], N. Nikiforou[11],
V. Nikolaenko[123,ad], I. Nikolic-Audit[135], K. Nikolopoulos[21], H. Nilsson[29], H.R. Nindhito[54], A. Nisati[73a],
N. Nishu[60c], R. Nisius[115], I. Nitsche[47], T. Nitta[179], T. Nobe[163], D.L. Noel[32], Y. Noguchi[86], I. Nomidis[135],
M.A. Nomura[29], M. Nordberg[36], J. Novak[92], T. Novak[92], O. Novgorodova[48], R. Novotny[141], L. Nozka[130],
K. Ntekas[171], E. Nurse[95], F.G. Oakham[34,ai], J. Ocariz[135], A. Ochi[83], I. Ochoa[39], J.P. Ochoa-Ricoux[146a],
K. O'Connor[26], S. Oda[88], S. Odaka[82], S. Oerdek[53], A. Ogrodnik[84a], A. Oh[101], C.C. Ohm[154], H. Oide[165],
M.L. Ojeda[167], H. Okawa[169], Y. Okazaki[86], M.W. O'Keefe[91], Y. Okumura[163], A. Olariu[27b],
L.F. Oleiro Seabra[139a], S.A. Olivares Pino[146a], D. Oliveira Damazio[29], J.L. Oliver[1], M.J.R. Olsson[171],
A. Olszewski[85], J. Olszowska[85], Ö.O. Öncel[24], D.C. O'Neil[152], A.P. O'neill[134], A. Onofre[139a,139e],
P.U.E. Onyisi[11], H. Oppen[133], R.G. Oreamuno Madriz[121], M.J. Oreglia[37], G.E. Orellana[89],
D. Orestano[75a,75b], N. Orlando[14], R.S. Orr[167], V. O'Shea[57], R. Ospanov[60a], G. Otero y Garzon[30],
H. Otono[88], P.S. Ott[61a], G.J. Ottino[18], M. Ouchrif[35d], J. Ouellette[29], F. Ould-Saada[133], A. Ouraou[144,*],
Q. Ouyang[15a], M. Owen[57], R.E. Owen[143], V.E. Ozcan[12c], N. Ozturk[8], J. Pacalt[130], H.A. Pacey[32],
K. Pachal[49], A. Pacheco Pages[14], C. Padilla Aranda[14], S. Pagan Griso[18], G. Palacino[66], S. Palazzo[50],
S. Palestini[36], M. Palka[84b], P. Palni[84a], C.E. Pandini[54], J.G. Panduro Vazquez[94], P. Pani[46],
G. Panizzo[67a,67c], L. Paolozzi[54], C. Papadatos[110], K. Papageorgiou[9,g], S. Parajuli[42], A. Paramonov[6],
C. Paraskevopoulos[10], D. Paredes Hernandez[63b], S.R. Paredes Saenz[134], B. Parida[180], T.H. Park[167],
A.J. Parker[31], M.A. Parker[32], F. Parodi[55b,55a], E.W. Parrish[121], J.A. Parsons[39], U. Parzefall[52],
L. Pascual Dominguez[135], V.R. Pascuzzi[18], J.M.P. Pasner[145], F. Pasquali[120], E. Pasqualucci[73a],
S. Passaggio[55b], F. Pastore[94], P. Pasuwan[45a,45b], S. Pataraia[100], J.R. Pater[101], A. Pathak[181,i], J. Patton[91],
T. Pauly[36], J. Pearkes[153], M. Pedersen[133], L. Pedraza Diaz[119], R. Pedro[139a], T. Peiffer[53],
S.V. Peleganchuk[122b,122a], O. Penc[140], C. Peng[63b], H. Peng[60a], B.S. Peralva[81a], M.M. Perego[65],
A.P. Pereira Peixoto[139a], L. Pereira Sanchez[45a,45b], D.V. Perepelitsa[29], E. Perez Codina[168a], F. Peri[19],
L. Perini[69a,69b], H. Pernegger[36], S. Perrella[36], A. Perrevoort[120], K. Peters[46], R.F.Y. Peters[101],
B.A. Petersen[36], T.C. Petersen[40], E. Petit[102], V. Petousis[141], C. Petridou[162], F. Petrucci[75a,75b], M. Pettee[183],
N.E. Pettersson[103], K. Petukhova[142], A. Peyaud[144], R. Pezoa[146d], L. Pezzotti[71a,71b], T. Pham[105],
P.W. Phillips[143], M.W. Phipps[173], G. Piacquadio[155], E. Pianori[18], A. Picazio[103], R.H. Pickles[101],
R. Piegaia[30], D. Pietreanu[27b], J.E. Pilcher[37], A.D. Pilkington[101], M. Pinamonti[67a,67c], J.L. Pinfold[3],

C. Pitman Donaldson[95], M. Pitt[161], L. Pizzimento[74a,74b], A. Pizzini[120], M.-A. Pleier[29], V. Plesanovs[52], V. Pleskot[142], E. Plotnikova[80], P. Podberezko[122b,122a], R. Poettgen[97], R. Poggi[54], L. Poggioli[135], I. Pogrebnyak[107], D. Pohl[24], I. Pokharel[53], G. Polesello[71a], A. Poley[152,168a], A. Policicchio[73a,73b], R. Polifka[142], A. Polini[23b], C.S. Pollard[46], V. Polychronakos[29], D. Ponomarenko[112], L. Pontecorvo[36], S. Popa[27a], G.A. Popeneciu[27d], L. Portales[5], D.M. Portillo Quintero[58], S. Pospisil[141], K. Potamianos[46], I.N. Potrap[80], C.J. Potter[32], H. Potti[11], T. Poulsen[97], J. Poveda[174], T.D. Powell[149], G. Pownall[46], M.E. Pozo Astigarraga[36], A. Prades Ibanez[174], P. Pralavorio[102], M.M. Prapa[44], S. Prell[79], D. Price[101], M. Primavera[68a], M.L. Proffitt[148], N. Proklova[112], K. Prokofiev[63c], F. Prokoshin[80], S. Protopopescu[29], J. Proudfoot[6], M. Przybycien[84a], D. Pudzha[137], A. Puri[173], P. Puzo[65], D. Pyatiizbyantseva[112], J. Qian[106], Y. Qin[101], A. Quadt[53], M. Queitsch-Maitland[36], M. Racko[28a], F. Ragusa[69a,69b], G. Rahal[98], J.A. Raine[54], S. Rajagopalan[29], A. Ramirez Morales[93], K. Ran[15a,15d], D.M. Rauch[46], F. Rauscher[114], S. Rave[100], B. Ravina[57], I. Ravinovich[180], J.H. Rawling[101], M. Raymond[36], A.L. Read[133], N.P. Readioff[149], M. Reale[68a,68b], D.M. Rebuzzi[71a,71b], G. Redlinger[29], K. Reeves[43], D. Reikher[161], A. Reiss[100], A. Rej[151], C. Rembser[36], A. Renardi[46], M. Renda[27b], M.B. Rendel[115], A.G. Rennie[57], S. Resconi[69a], E.D. Resseguie[18], S. Rettie[95], B. Reynolds[127], E. Reynolds[21], O.L. Rezanova[122b,122a], P. Reznicek[142], E. Ricci[76a,76b], R. Richter[115], S. Richter[46], E. Richter-Was[84b], M. Ridel[135], P. Rieck[115], O. Rifki[46], M. Rijssenbeek[155], A. Rimoldi[71a,71b], M. Rimoldi[46], L. Rinaldi[23b], T.T. Rinn[173], G. Ripellino[154], I. Riu[14], P. Rivadeneira[46], J.C. Rivera Vergara[176], F. Rizatdinova[129], E. Rizvi[93], C. Rizzi[36], S.H. Robertson[104,z], M. Robin[46], D. Robinson[32], C.M. Robles Gajardo[146d], M. Robles Manzano[100], A. Robson[57], A. Rocchi[74a,74b], C. Roda[72a,72b], S. Rodriguez Bosca[174], A. Rodriguez Rodriguez[52], A.M. Rodríguez Vera[168b], S. Roe[36], J. Roggel[182], O. Røhne[133], R. Röhrig[115], R.A. Rojas[146d], B. Roland[52], C.P.A. Roland[66], J. Roloff[29], A. Romaniouk[112], M. Romano[23b,23a], N. Rompotis[91], M. Ronzani[125], L. Roos[135], S. Rosati[73a], G. Rosin[103], B.J. Rosser[36], E. Rossi[46], E. Rossi[75a,75b], E. Rossi[70a,70b], L.P. Rossi[55b], L. Rossini[46], R. Rosten[14], M. Rotaru[27b], B. Rottler[52], D. Rousseau[65], G. Rovelli[71a,71b], A. Roy[11], D. Roy[33e], A. Rozanov[102], Y. Rozen[160], X. Ruan[33e], T.A. Ruggeri[1], F. Rühr[52], A. Ruiz-Martinez[174], A. Rummler[36], Z. Rurikova[52], N.A. Rusakovich[80], H.L. Russell[104], L. Rustige[38,47], J.P. Rutherfoord[7], E.M. Rüttinger[149], M. Rybar[142], G. Rybkin[65], E.B. Rye[133], A. Ryzhov[123], J.A. Sabater Iglesias[46], P. Sabatini[174], L. Sabetta[73a,73b], S. Sacerdoti[65], H.F-W. Sadrozinski[145], R. Sadykov[80], F. Safai Tehrani[73a], B. Safarzadeh Samani[156], M. Safdari[153], P. Saha[121], S. Saha[104], M. Sahinsoy[115], A. Sahu[182], M. Saimpert[36], M. Saito[163], T. Saito[163], H. Sakamoto[163], D. Salamani[54], G. Salamanna[75a,75b], A. Salnikov[153], J. Salt[174], A. Salvador Salas[14], D. Salvatore[41b,41a], F. Salvatore[156], A. Salvucci[63a], A. Salzburger[36], J. Samarati[36], D. Sammel[52], D. Sampsonidis[162], D. Sampsonidou[60d,60c], J. Sánchez[174], A. Sanchez Pineda[67a,36,67c], H. Sandaker[133], C.O. Sander[46], I.G. Sanderswood[90], M. Sandhoff[182], C. Sandoval[22b], D.P.C. Sankey[143], M. Sannino[55b,55a], Y. Sano[117], A. Sansoni[51], C. Santoni[38], H. Santos[139a,139b], S.N. Santpur[18], A. Santra[174], K.A. Saoucha[149], A. Sapronov[80], J.G. Saraiva[139a,139d], O. Sasaki[82], K. Sato[169], F. Sauerburger[52], E. Sauvan[5], P. Savard[167,ai], R. Sawada[163], C. Sawyer[143], L. Sawyer[96], I. Sayago Galvan[174], C. Sbarra[23b], A. Sbrizzi[67a,67c], T. Scanlon[95], J. Schaarschmidt[148], P. Schacht[115], D. Schaefer[37], L. Schaefer[136], U. Schäfer[100], A.C. Schaffer[65], D. Schaile[114], R.D. Schamberger[155], E. Schanet[114], C. Scharf[19], N. Scharmberg[101], V.A. Schegelsky[137], D. Scheirich[142], F. Schenck[19], M. Schernau[171], C. Schiavi[55b,55a], L.K. Schildgen[24], Z.M. Schillaci[26], E.J. Schioppa[68a,68b], M. Schioppa[41b,41a], K.E. Schleicher[52], S. Schlenker[36], K.R. Schmidt-Sommerfeld[115], K. Schmieden[100], C. Schmitt[100], S. Schmitt[46], L. Schoeffel[144], A. Schoening[61b], P.G. Scholer[52], E. Schopf[134], M. Schott[100], J.F.P. Schouwenberg[119], J. Schovancova[36], S. Schramm[54], F. Schroeder[182], A. Schulte[100], H-C. Schultz-Coulon[61a], M. Schumacher[52], B.A. Schumm[145], Ph. Schune[144], A. Schwartzman[153], T.A. Schwarz[106], Ph. Schwemling[144], R. Schwienhorst[107], A. Sciandra[145], G. Sciolla[26], M. Scornajenghi[41b,41a], F. Scuri[72a], F. Scutti[105], L.M. Scyboz[115], C.D. Sebastiani[91], K. Sedlaczek[47], P. Seema[19], S.C. Seidel[118], A. Seiden[145], B.D. Seidlitz[29], T. Seiss[37], C. Seitz[46],

J.M. Seixas[81b], G. Sekhniaidze[70a], S.J. Sekula[42], N. Semprini-Cesari[23b,23a], S. Sen[49], C. Serfon[29],
L. Serin[65], L. Serkin[67a,67b], M. Sessa[60a], H. Severini[128], S. Sevova[153], F. Sforza[55b,55a], A. Sfyrla[54],
E. Shabalina[53], J.D. Shahinian[136], N.W. Shaikh[45a,45b], D. Shaked Renous[180], L.Y. Shan[15a], M. Shapiro[18],
A. Sharma[36], A.S. Sharma[1], P.B. Shatalov[124], K. Shaw[156], S.M. Shaw[101], M. Shehade[180], Y. Shen[128],
A.D. Sherman[25], P. Sherwood[95], L. Shi[95], C.O. Shimmin[183], Y. Shimogama[179], M. Shimojima[116],
J.D. Shinner[94], I.P.J. Shipsey[134], S. Shirabe[165], M. Shiyakova[80,x], J. Shlomi[180], A. Shmeleva[111],
M.J. Shochet[37], J. Shojaii[105], D.R. Shope[154], S. Shrestha[127], E.M. Shrif[33e], M.J. Shroff[176], E. Shulga[180],
P. Sicho[140], A.M. Sickles[173], E. Sideras Haddad[33e], O. Sidiropoulou[36], A. Sidoti[23b,23a], F. Siegert[48],
Dj. Sijacki[16], M.Jr. Silva[181], M.V. Silva Oliveira[36], S.B. Silverstein[45a], S. Simion[65], R. Simoniello[100],
C.J. Simpson-allsop[21], S. Simsek[12b], P. Sinervo[167], V. Sinetckii[113], S. Singh[152], M. Sioli[23b,23a], I. Siral[131],
S.Yu. Sivoklokov[113], J. Sjölin[45a,45b], A. Skaf[53], E. Skorda[97], P. Skubic[128], M. Slawinska[85], K. Sliwa[170],
R. Slovak[142], V. Smakhtin[180], B.H. Smart[143], J. Smiesko[28b], N. Smirnov[112], S.Yu. Smirnov[112],
Y. Smirnov[112], L.N. Smirnova[113,r], O. Smirnova[97], E.A. Smith[37], H.A. Smith[134], M. Smizanska[90],
K. Smolek[141], A. Smykiewicz[85], A.A. Snesarev[111], H.L. Snoek[120], I.M. Snyder[131], S. Snyder[29],
R. Sobie[176,z], A. Soffer[161], A. Søgaard[50], F. Sohns[53], C.A. Solans Sanchez[36], E.Yu. Soldatov[112],
U. Soldevila[174], A.A. Solodkov[123], A. Soloshenko[80], O.V. Solovyanov[123], V. Solovyev[137], P. Sommer[149],
H. Son[170], A. Sonay[14], W. Song[143], W.Y. Song[168b], A. Sopczak[141], A.L. Sopio[95], F. Sopkova[28b],
S. Sottocornola[71a,71b], R. Soualah[67a,67c], A.M. Soukharev[122b,122a], D. South[46], S. Spagnolo[68a,68b],
M. Spalla[115], M. Spangenberg[178], F. Spanò[94], D. Sperlich[52], T.M. Spieker[61a], G. Spigo[36], M. Spina[156],
D.P. Spiteri[57], M. Spousta[142], A. Stabile[69a,69b], B.L. Stamas[121], R. Stamen[61a], M. Stamenkovic[120],
A. Stampekis[21], E. Stanecka[85], B. Stanislaus[134], M.M. Stanitzki[46], M. Stankaityte[134], B. Stapf[120],
E.A. Starchenko[123], G.H. Stark[145], J. Stark[58], P. Staroba[140], P. Starovoitov[61a], S. Stärz[104], R. Staszewski[85],
G. Stavropoulos[44], M. Stegler[46], P. Steinberg[29], A.L. Steinhebel[131], B. Stelzer[152,168a], H.J. Stelzer[138],
O. Stelzer-Chilton[168a], H. Stenzel[56], T.J. Stevenson[156], G.A. Stewart[36], M.C. Stockton[36], G. Stoicea[27b],
M. Stolarski[139a], S. Stonjek[115], A. Straessner[48], J. Strandberg[154], S. Strandberg[45a,45b], M. Strauss[128],
T. Strebler[102], P. Strizenec[28b], R. Ströhmer[177], D.M. Strom[131], R. Stroynowski[42], A. Strubig[45a,45b],
S.A. Stucci[29], B. Stugu[17], J. Stupak[128], N.A. Styles[46], D. Su[153], W. Su[60c,148], X. Su[60a], N.B. Suarez[138],
V.V. Sulin[111], M.J. Sullivan[91], D.M.S. Sultan[54], S. Sultansoy[4c], T. Sumida[86], S. Sun[106], X. Sun[101],
C.J.E. Suster[157], M.R. Sutton[156], S. Suzuki[82], M. Svatos[140], M. Swiatlowski[168a], S.P. Swift[2], T. Swirski[177],
A. Sydorenko[100], I. Sykora[28a], M. Sykora[142], T. Sykora[142], D. Ta[100], K. Tackmann[46,w], J. Taenzer[161],
A. Taffard[171], R. Tafirout[168a], E. Tagiev[123], R.H.M. Taibah[135], R. Takashima[87], K. Takeda[83],
T. Takeshita[150], E.P. Takeva[50], Y. Takubo[82], M. Talby[102], A.A. Talyshev[122b,122a], K.C. Tam[63b],
N.M. Tamir[161], J. Tanaka[163], R. Tanaka[65], S. Tapia Araya[173], S. Tapprogge[100],
A. Tarek Abouelfadl Mohamed[107], S. Tarem[160], K. Tariq[60b], G. Tarna[27b,d], G.F. Tartarelli[69a], P. Tas[142],
M. Tasevsky[140], E. Tassi[41b,41a], A. Tavares Delgado[139a], Y. Tayalati[35e], A.J. Taylor[50], G.N. Taylor[105],
W. Taylor[168b], H. Teagle[91], A.S. Tee[90], R. Teixeira De Lima[153], P. Teixeira-Dias[94], H. Ten Kate[36],
J.J. Teoh[120], K. Terashi[163], J. Terron[99], S. Terzo[14], M. Testa[51], R.J. Teuscher[167,z], S.J. Thais[183],
N. Themistokleous[50], T. Theveneaux-Pelzer[19], F. Thiele[40], D.W. Thomas[94], J.O. Thomas[42], J.P. Thomas[21],
E.A. Thompson[46], P.D. Thompson[21], E. Thomson[136], E.J. Thorpe[93], V.O. Tikhomirov[111,ae],
Yu.A. Tikhonov[122b,122a], S. Timoshenko[112], P. Tipton[183], S. Tisserant[102], K. Todome[23b,23a],
S. Todorova-Nova[142], S. Todt[48], J. Tojo[88], S. Tokár[28a], K. Tokushuku[82], E. Tolley[127], R. Tombs[32],
K.G. Tomiwa[33e], M. Tomoto[82,117], L. Tompkins[153], P. Tornambe[103], E. Torrence[131], H. Torres[48],
E. Torró Pastor[174], M. Toscani[30], C. Tosciri[134], J. Toth[102,y], D.R. Tovey[149], A. Traeet[17], C.J. Treado[125],
T. Trefzger[177], F. Tresoldi[156], A. Tricoli[29], I.M. Trigger[168a], S. Trincaz-Duvoid[135], D.A. Trischuk[175],
W. Trischuk[167], B. Trocmé[58], A. Trofymov[65], C. Troncon[69a], F. Trovato[156], L. Truong[33c], M. Trzebinski[85],
A. Trzupek[85], F. Tsai[46], J.C-L. Tseng[134], P.V. Tsiareshka[108,ac], A. Tsirigotis[162,u], V. Tsiskaridze[155],
E.G. Tskhadadze[159a], M. Tsopoulou[162], I.I. Tsukerman[124], V. Tsulaia[18], S. Tsuno[82], D. Tsybychev[155],

36

Y. Tu[63b], A. Tudorache[27b], V. Tudorache[27b], T.T. Tulbure[27a], A.N. Tuna[59], S. Turchikhin[80], D. Turgeman[180], I. Turk Cakir[4b,s], R.J. Turner[21], R. Turra[69a], P.M. Tuts[39], S. Tzamarias[162], E. Tzovara[100], K. Uchida[163], F. Ukegawa[169], G. Unal[36], M. Unal[11], A. Undrus[29], G. Unel[171], F.C. Ungaro[105], Y. Unno[82], K. Uno[163], J. Urban[28b], P. Urquijo[105], G. Usai[8], Z. Uysal[12d], V. Vacek[141], B. Vachon[104], K.O.H. Vadla[133], T. Vafeiadis[36], A. Vaidya[95], C. Valderanis[114], E. Valdes Santurio[45a,45b], M. Valente[168a], S. Valentinetti[23b,23a], A. Valero[174], L. Valéry[46], R.A. Vallance[21], A. Vallier[36], J.A. Valls Ferrer[174], T.R. Van Daalen[14], P. Van Gemmeren[6], S. Van Stroud[95], I. Van Vulpen[120], M. Vanadia[74a,74b], W. Vandelli[36], M. Vandenbroucke[144], E.R. Vandewall[129], A. Vaniachine[166], D. Vannicola[73a,73b], R. Vari[73a], E.W. Varnes[7], C. Varni[55b,55a], T. Varol[158], D. Varouchas[65], K.E. Varvell[157], M.E. Vasile[27b], G.A. Vasquez[176], F. Vazeille[38], D. Vazquez Furelos[14], T. Vazquez Schroeder[36], J. Veatch[53], V. Vecchio[101], M.J. Veen[120], L.M. Veloce[167], F. Veloso[139a,139c], S. Veneziano[73a], A. Ventura[68a,68b], A. Verbytskyi[115], V. Vercesi[71a], M. Verducci[72a,72b], C.M. Vergel Infante[79], C. Vergis[24], W. Verkerke[120], A.T. Vermeulen[120], J.C. Vermeulen[120], C. Vernieri[153], P.J. Verschuuren[94], M.C. Vetterli[152,ai], N. Viaux Maira[146d], T. Vickey[149], O.E. Vickey Boeriu[149], G.H.A. Viehhauser[134], L. Vigani[61b], M. Villa[23b,23a], M. Villaplana Perez[3], E.M. Villhauer[50], E. Vilucchi[51], M.G. Vincter[34], G.S. Virdee[21], A. Vishwakarma[50], C. Vittori[23b,23a], I. Vivarelli[156], M. Vogel[182], P. Vokac[141], S.E. von Buddenbrock[33e], E. Von Toerne[24], V. Vorobel[142], K. Vorobev[112], M. Vos[174], J.H. Vossebeld[91], M. Vozak[101], N. Vranjes[16], M. Vranjes Milosavljevic[16], V. Vrba[141], M. Vreeswijk[120], N.K. Vu[102], R. Vuillermet[36], I. Vukotic[37], S. Wada[169], P. Wagner[24], W. Wagner[182], J. Wagner-Kuhr[114], S. Wahdan[182], H. Wahlberg[89], R. Wakasa[169], V.M. Walbrecht[115], J. Walder[143], R. Walker[114], S.D. Walker[94], W. Walkowiak[151], V. Wallangen[45a,45b], A.M. Wang[59], A.Z. Wang[181], C. Wang[60a], C. Wang[60c], H. Wang[18], H. Wang[3], J. Wang[63a], P. Wang[42], Q. Wang[128], R.-J. Wang[100], R. Wang[60a], R. Wang[6], S.M. Wang[158], W.T. Wang[60a], W. Wang[15c], W.X. Wang[60a], Y. Wang[60a], Z. Wang[106], C. Wanotayaroj[46], A. Warburton[104], C.P. Ward[32], R.J. Ward[21], N. Warrack[57], A.T. Watson[21], M.F. Watson[21], G. Watts[148], B.M. Waugh[95], A.F. Webb[11], C. Weber[29], M.S. Weber[20], S.A. Weber[34], S.M. Weber[61a], A.R. Weidberg[134], J. Weingarten[47], M. Weirich[100], C. Weiser[52], P.S. Wells[36], T. Wenaus[29], B. Wendland[47], T. Wengler[36], S. Wenig[36], N. Wermes[24], M. Wessels[61a], T.D. Weston[20], K. Whalen[131], A.M. Wharton[90], A.S. White[106], A. White[8], M.J. White[1], D. Whiteson[171], B.W. Whitmore[90], W. Wiedenmann[181], C. Wiel[48], M. Wielers[143], N. Wieseotte[100], C. Wiglesworth[40], L.A.M. Wiik-Fuchs[52], H.G. Wilkens[36], L.J. Wilkins[94], D.M. Williams[39], H.H. Williams[136], S. Williams[32], S. Willocq[103], P.J. Windischhofer[134], I. Wingerter-Seez[5], E. Winkels[156], F. Winklmeier[131], B.T. Winter[52], M. Wittgen[153], M. Wobisch[96], A. Wolf[100], R. Wölker[134], J. Wollrath[52], M.W. Wolter[85], H. Wolters[139a,139c], V.W.S. Wong[175], A.F. Wongel[46], N.L. Woods[145], S.D. Worm[46], B.K. Wosiek[85], K.W. Woźniak[85], K. Wraight[57], S.L. Wu[181], X. Wu[54], Y. Wu[60a], J. Wuerzinger[134], T.R. Wyatt[101], B.M. Wynne[50], S. Xella[40], L. Xia[178], J. Xiang[63c], X. Xiao[106], X. Xie[60a], I. Xiotidis[156], D. Xu[15a], H. Xu[60a], H. Xu[60a], L. Xu[29], R. Xu[136], T. Xu[144], W. Xu[106], Y. Xu[15b], Z. Xu[60b], Z. Xu[153], B. Yabsley[157], S. Yacoob[33a], D.P. Yallup[95], N. Yamaguchi[88], Y. Yamaguchi[165], A. Yamamoto[82], M. Yamatani[163], T. Yamazaki[163], Y. Yamazaki[83], J. Yan[60c], Z. Yan[25], H.J. Yang[60c,60d], H.T. Yang[18], S. Yang[60a], T. Yang[63c], X. Yang[60a], X. Yang[60b,58], Y. Yang[163], Z. Yang[60a], W-M. Yao[18], Y.C. Yap[46], E. Yatsenko[60c], H. Ye[15c], J. Ye[42], S. Ye[29], I. Yeletskikh[80], M.R. Yexley[90], E. Yigitbasi[25], P. Yin[39], K. Yorita[179], K. Yoshihara[79], C.J.S. Young[36], C. Young[153], J. Yu[79], R. Yuan[60b,h], X. Yue[61a], M. Zaazoua[35e], B. Zabinski[85], G. Zacharis[10], E. Zaffaroni[54], J. Zahreddine[135], A.M. Zaitsev[123,ad], T. Zakareishvili[159b], N. Zakharchuk[34], S. Zambito[36], D. Zanzi[36], S.V. Zeißner[47], C. Zeitnitz[182], G. Zemaityte[134], J.C. Zeng[173], O. Zenin[123], T. Ženiš[28a], D. Zerwas[65], M. Zgubič[134], B. Zhang[15c], D.F. Zhang[15b], G. Zhang[15b], J. Zhang[60b], J. Zhang[6], Kaili. Zhang[15a], L. Zhang[15c], L. Zhang[60a], M. Zhang[173], R. Zhang[181], S. Zhang[106], X. Zhang[60c], X. Zhang[60b], Y. Zhang[15a,15d], Z. Zhang[63a], Z. Zhang[65], P. Zhao[49], Y. Zhao[145], Z. Zhao[60a], A. Zhemchugov[80], Z. Zheng[106], D. Zhong[173], B. Zhou[106], C. Zhou[181], H. Zhou[7], M.S. Zhou[15a,15d], M. Zhou[155], N. Zhou[60c], Y. Zhou[7], C.G. Zhu[60b], C. Zhu[15a,15d], H.L. Zhu[60a], H. Zhu[15a], J. Zhu[106], Y. Zhu[60a], X. Zhuang[15a], K. Zhukov[111],

V. Zhulanov[122b,122a], D. Zieminska[66], N.I. Zimine[80], S. Zimmermann[52], Z. Zinonos[115], M. Ziolkowski[151], L. Živković[16], G. Zobernig[181], A. Zoccoli[23b,23a], K. Zoch[53], T.G. Zorbas[149], R. Zou[37], L. Zwalinski[36].

[1]Department of Physics, University of Adelaide, Adelaide; Australia.

[2]Physics Department, SUNY Albany, Albany NY; United States of America.

[3]Department of Physics, University of Alberta, Edmonton AB; Canada.

[4][a]Department of Physics, Ankara University, Ankara;[b]Istanbul Aydin University, Application and Research Center for Advanced Studies, Istanbul;[c]Division of Physics, TOBB University of Economics and Technology, Ankara; Turkey.

[5]LAPP, Université Grenoble Alpes, Université Savoie Mont Blanc, CNRS/IN2P3, Annecy; France.

[6]High Energy Physics Division, Argonne National Laboratory, Argonne IL; United States of America.

[7]Department of Physics, University of Arizona, Tucson AZ; United States of America.

[8]Department of Physics, University of Texas at Arlington, Arlington TX; United States of America.

[9]Physics Department, National and Kapodistrian University of Athens, Athens; Greece.

[10]Physics Department, National Technical University of Athens, Zografou; Greece.

[11]Department of Physics, University of Texas at Austin, Austin TX; United States of America.

[12][a]Bahcesehir University, Faculty of Engineering and Natural Sciences, Istanbul;[b]Istanbul Bilgi University, Faculty of Engineering and Natural Sciences, Istanbul;[c]Department of Physics, Bogazici University, Istanbul;[d]Department of Physics Engineering, Gaziantep University, Gaziantep; Turkey.

[13]Institute of Physics, Azerbaijan Academy of Sciences, Baku; Azerbaijan.

[14]Institut de Física d'Altes Energies (IFAE), Barcelona Institute of Science and Technology, Barcelona; Spain.

[15][a]Institute of High Energy Physics, Chinese Academy of Sciences, Beijing;[b]Physics Department, Tsinghua University, Beijing;[c]Department of Physics, Nanjing University, Nanjing;[d]University of Chinese Academy of Science (UCAS), Beijing; China.

[16]Institute of Physics, University of Belgrade, Belgrade; Serbia.

[17]Department for Physics and Technology, University of Bergen, Bergen; Norway.

[18]Physics Division, Lawrence Berkeley National Laboratory and University of California, Berkeley CA; United States of America.

[19]Institut für Physik, Humboldt Universität zu Berlin, Berlin; Germany.

[20]Albert Einstein Center for Fundamental Physics and Laboratory for High Energy Physics, University of Bern, Bern; Switzerland.

[21]School of Physics and Astronomy, University of Birmingham, Birmingham; United Kingdom.

[22][a]Facultad de Ciencias y Centro de Investigaciónes, Universidad Antonio Nariño, Bogotá;[b]Departamento de Física, Universidad Nacional de Colombia, Bogotá, Colombia; Colombia.

[23][a]INFN Bologna and Universita' di Bologna, Dipartimento di Fisica;[b]INFN Sezione di Bologna; Italy.

[24]Physikalisches Institut, Universität Bonn, Bonn; Germany.

[25]Department of Physics, Boston University, Boston MA; United States of America.

[26]Department of Physics, Brandeis University, Waltham MA; United States of America.

[27][a]Transilvania University of Brasov, Brasov;[b]Horia Hulubei National Institute of Physics and Nuclear Engineering, Bucharest;[c]Department of Physics, Alexandru Ioan Cuza University of Iasi, Iasi;[d]National Institute for Research and Development of Isotopic and Molecular Technologies, Physics Department, Cluj-Napoca;[e]University Politehnica Bucharest, Bucharest;[f]West University in Timisoara, Timisoara; Romania.

[28][a]Faculty of Mathematics, Physics and Informatics, Comenius University, Bratislava;[b]Department of Subnuclear Physics, Institute of Experimental Physics of the Slovak Academy of Sciences, Kosice; Slovak Republic.

[29]Physics Department, Brookhaven National Laboratory, Upton NY; United States of America.

[30]Departamento de Física, Universidad de Buenos Aires, Buenos Aires; Argentina.

[31]California State University, CA; United States of America.

[32]Cavendish Laboratory, University of Cambridge, Cambridge; United Kingdom.

[33][a]Department of Physics, University of Cape Town, Cape Town;[b]iThemba Labs, Western Cape;[c]Department of Mechanical Engineering Science, University of Johannesburg, Johannesburg;[d]University of South Africa, Department of Physics, Pretoria;[e]School of Physics, University of the Witwatersrand, Johannesburg; South Africa.

[34]Department of Physics, Carleton University, Ottawa ON; Canada.

[35][a]Faculté des Sciences Ain Chock, Réseau Universitaire de Physique des Hautes Energies - Université Hassan II, Casablanca;[b]Faculté des Sciences, Université Ibn-Tofail, Kénitra;[c]Faculté des Sciences Semlalia, Université Cadi Ayyad, LPHEA-Marrakech;[d]Faculté des Sciences, Université Mohamed Premier and LPTPM, Oujda;[e]Faculté des sciences, Université Mohammed V, Rabat; Morocco.

[36]CERN, Geneva; Switzerland.

[37]Enrico Fermi Institute, University of Chicago, Chicago IL; United States of America.

[38]LPC, Université Clermont Auvergne, CNRS/IN2P3, Clermont-Ferrand; France.

[39]Nevis Laboratory, Columbia University, Irvington NY; United States of America.

[40]Niels Bohr Institute, University of Copenhagen, Copenhagen; Denmark.

[41][a]Dipartimento di Fisica, Università della Calabria, Rende;[b]INFN Gruppo Collegato di Cosenza, Laboratori Nazionali di Frascati; Italy.

[42]Physics Department, Southern Methodist University, Dallas TX; United States of America.

[43]Physics Department, University of Texas at Dallas, Richardson TX; United States of America.

[44]National Centre for Scientific Research "Demokritos", Agia Paraskevi; Greece.

[45][a]Department of Physics, Stockholm University;[b]Oskar Klein Centre, Stockholm; Sweden.

[46]Deutsches Elektronen-Synchrotron DESY, Hamburg and Zeuthen; Germany.

[47]Lehrstuhl für Experimentelle Physik IV, Technische Universität Dortmund, Dortmund; Germany.

[48]Institut für Kern- und Teilchenphysik, Technische Universität Dresden, Dresden; Germany.

[49]Department of Physics, Duke University, Durham NC; United States of America.

[50]SUPA - School of Physics and Astronomy, University of Edinburgh, Edinburgh; United Kingdom.

[51]INFN e Laboratori Nazionali di Frascati, Frascati; Italy.

[52]Physikalisches Institut, Albert-Ludwigs-Universität Freiburg, Freiburg; Germany.

[53]II. Physikalisches Institut, Georg-August-Universität Göttingen, Göttingen; Germany.

[54]Département de Physique Nucléaire et Corpusculaire, Université de Genève, Genève; Switzerland.

[55][a]Dipartimento di Fisica, Università di Genova, Genova;[b]INFN Sezione di Genova; Italy.

[56]II. Physikalisches Institut, Justus-Liebig-Universität Giessen, Giessen; Germany.

[57]SUPA - School of Physics and Astronomy, University of Glasgow, Glasgow; United Kingdom.

[58]LPSC, Université Grenoble Alpes, CNRS/IN2P3, Grenoble INP, Grenoble; France.

[59]Laboratory for Particle Physics and Cosmology, Harvard University, Cambridge MA; United States of America.

[60][a]Department of Modern Physics and State Key Laboratory of Particle Detection and Electronics, University of Science and Technology of China, Hefei;[b]Institute of Frontier and Interdisciplinary Science and Key Laboratory of Particle Physics and Particle Irradiation (MOE), Shandong University, Qingdao;[c]School of Physics and Astronomy, Shanghai Jiao Tong University, KLPPAC-MoE, SKLPPC, Shanghai;[d]Tsung-Dao Lee Institute, Shanghai; China.

[61][a]Kirchhoff-Institut für Physik, Ruprecht-Karls-Universität Heidelberg, Heidelberg;[b]Physikalisches Institut, Ruprecht-Karls-Universität Heidelberg, Heidelberg; Germany.

[62]Faculty of Applied Information Science, Hiroshima Institute of Technology, Hiroshima; Japan.

[63](a)Department of Physics, Chinese University of Hong Kong, Shatin, N.T., Hong Kong;(b)Department of Physics, University of Hong Kong, Hong Kong;(c)Department of Physics and Institute for Advanced Study, Hong Kong University of Science and Technology, Clear Water Bay, Kowloon, Hong Kong; China.

[64]Department of Physics, National Tsing Hua University, Hsinchu; Taiwan.

[65]IJCLab, Université Paris-Saclay, CNRS/IN2P3, 91405, Orsay; France.

[66]Department of Physics, Indiana University, Bloomington IN; United States of America.

[67](a)INFN Gruppo Collegato di Udine, Sezione di Trieste, Udine;(b)ICTP, Trieste;(c)Dipartimento Politecnico di Ingegneria e Architettura, Università di Udine, Udine; Italy.

[68](a)INFN Sezione di Lecce;(b)Dipartimento di Matematica e Fisica, Università del Salento, Lecce; Italy.

[69](a)INFN Sezione di Milano;(b)Dipartimento di Fisica, Università di Milano, Milano; Italy.

[70](a)INFN Sezione di Napoli;(b)Dipartimento di Fisica, Università di Napoli, Napoli; Italy.

[71](a)INFN Sezione di Pavia;(b)Dipartimento di Fisica, Università di Pavia, Pavia; Italy.

[72](a)INFN Sezione di Pisa;(b)Dipartimento di Fisica E. Fermi, Università di Pisa, Pisa; Italy.

[73](a)INFN Sezione di Roma;(b)Dipartimento di Fisica, Sapienza Università di Roma, Roma; Italy.

[74](a)INFN Sezione di Roma Tor Vergata;(b)Dipartimento di Fisica, Università di Roma Tor Vergata, Roma; Italy.

[75](a)INFN Sezione di Roma Tre;(b)Dipartimento di Matematica e Fisica, Università Roma Tre, Roma; Italy.

[76](a)INFN-TIFPA;(b)Università degli Studi di Trento, Trento; Italy.

[77]Institut für Astro- und Teilchenphysik, Leopold-Franzens-Universität, Innsbruck; Austria.

[78]University of Iowa, Iowa City IA; United States of America.

[79]Department of Physics and Astronomy, Iowa State University, Ames IA; United States of America.

[80]Joint Institute for Nuclear Research, Dubna; Russia.

[81](a)Departamento de Engenharia Elétrica, Universidade Federal de Juiz de Fora (UFJF), Juiz de Fora;(b)Universidade Federal do Rio De Janeiro COPPE/EE/IF, Rio de Janeiro;(c)Instituto de Física, Universidade de São Paulo, São Paulo; Brazil.

[82]KEK, High Energy Accelerator Research Organization, Tsukuba; Japan.

[83]Graduate School of Science, Kobe University, Kobe; Japan.

[84](a)AGH University of Science and Technology, Faculty of Physics and Applied Computer Science, Krakow;(b)Marian Smoluchowski Institute of Physics, Jagiellonian University, Krakow; Poland.

[85]Institute of Nuclear Physics Polish Academy of Sciences, Krakow; Poland.

[86]Faculty of Science, Kyoto University, Kyoto; Japan.

[87]Kyoto University of Education, Kyoto; Japan.

[88]Research Center for Advanced Particle Physics and Department of Physics, Kyushu University, Fukuoka ; Japan.

[89]Instituto de Física La Plata, Universidad Nacional de La Plata and CONICET, La Plata; Argentina.

[90]Physics Department, Lancaster University, Lancaster; United Kingdom.

[91]Oliver Lodge Laboratory, University of Liverpool, Liverpool; United Kingdom.

[92]Department of Experimental Particle Physics, Jožef Stefan Institute and Department of Physics, University of Ljubljana, Ljubljana; Slovenia.

[93]School of Physics and Astronomy, Queen Mary University of London, London; United Kingdom.

[94]Department of Physics, Royal Holloway University of London, Egham; United Kingdom.

[95]Department of Physics and Astronomy, University College London, London; United Kingdom.

[96]Louisiana Tech University, Ruston LA; United States of America.

[97]Fysiska institutionen, Lunds universitet, Lund; Sweden.

[98]Centre de Calcul de l'Institut National de Physique Nucléaire et de Physique des Particules (IN2P3), Villeurbanne; France.

[99] Departamento de Física Teorica C-15 and CIAFF, Universidad Autónoma de Madrid, Madrid; Spain.

[100] Institut für Physik, Universität Mainz, Mainz; Germany.

[101] School of Physics and Astronomy, University of Manchester, Manchester; United Kingdom.

[102] CPPM, Aix-Marseille Université, CNRS/IN2P3, Marseille; France.

[103] Department of Physics, University of Massachusetts, Amherst MA; United States of America.

[104] Department of Physics, McGill University, Montreal QC; Canada.

[105] School of Physics, University of Melbourne, Victoria; Australia.

[106] Department of Physics, University of Michigan, Ann Arbor MI; United States of America.

[107] Department of Physics and Astronomy, Michigan State University, East Lansing MI; United States of America.

[108] B.I. Stepanov Institute of Physics, National Academy of Sciences of Belarus, Minsk; Belarus.

[109] Research Institute for Nuclear Problems of Byelorussian State University, Minsk; Belarus.

[110] Group of Particle Physics, University of Montreal, Montreal QC; Canada.

[111] P.N. Lebedev Physical Institute of the Russian Academy of Sciences, Moscow; Russia.

[112] National Research Nuclear University MEPhI, Moscow; Russia.

[113] D.V. Skobeltsyn Institute of Nuclear Physics, M.V. Lomonosov Moscow State University, Moscow; Russia.

[114] Fakultät für Physik, Ludwig-Maximilians-Universität München, München; Germany.

[115] Max-Planck-Institut für Physik (Werner-Heisenberg-Institut), München; Germany.

[116] Nagasaki Institute of Applied Science, Nagasaki; Japan.

[117] Graduate School of Science and Kobayashi-Maskawa Institute, Nagoya University, Nagoya; Japan.

[118] Department of Physics and Astronomy, University of New Mexico, Albuquerque NM; United States of America.

[119] Institute for Mathematics, Astrophysics and Particle Physics, Radboud University Nijmegen/Nikhef, Nijmegen; Netherlands.

[120] Nikhef National Institute for Subatomic Physics and University of Amsterdam, Amsterdam; Netherlands.

[121] Department of Physics, Northern Illinois University, DeKalb IL; United States of America.

[122] $^{(a)}$Budker Institute of Nuclear Physics and NSU, SB RAS, Novosibirsk; $^{(b)}$Novosibirsk State University Novosibirsk; Russia.

[123] Institute for High Energy Physics of the National Research Centre Kurchatov Institute, Protvino; Russia.

[124] Institute for Theoretical and Experimental Physics named by A.I. Alikhanov of National Research Centre "Kurchatov Institute", Moscow; Russia.

[125] Department of Physics, New York University, New York NY; United States of America.

[126] Ochanomizu University, Otsuka, Bunkyo-ku, Tokyo; Japan.

[127] Ohio State University, Columbus OH; United States of America.

[128] Homer L. Dodge Department of Physics and Astronomy, University of Oklahoma, Norman OK; United States of America.

[129] Department of Physics, Oklahoma State University, Stillwater OK; United States of America.

[130] Palacký University, RCPTM, Joint Laboratory of Optics, Olomouc; Czech Republic.

[131] Institute for Fundamental Science, University of Oregon, Eugene, OR; United States of America.

[132] Graduate School of Science, Osaka University, Osaka; Japan.

[133] Department of Physics, University of Oslo, Oslo; Norway.

[134] Department of Physics, Oxford University, Oxford; United Kingdom.

[135] LPNHE, Sorbonne Université, Université de Paris, CNRS/IN2P3, Paris; France.

[136] Department of Physics, University of Pennsylvania, Philadelphia PA; United States of America.

[137] Konstantinov Nuclear Physics Institute of National Research Centre "Kurchatov Institute", PNPI, St.

Petersburg; Russia.

[138]Department of Physics and Astronomy, University of Pittsburgh, Pittsburgh PA; United States of America.

[139][(a)]Laboratório de Instrumentação e Física Experimental de Partículas - LIP, Lisboa;[(b)]Departamento de Física, Faculdade de Ciências, Universidade de Lisboa, Lisboa;[(c)]Departamento de Física, Universidade de Coimbra, Coimbra;[(d)]Centro de Física Nuclear da Universidade de Lisboa, Lisboa;[(e)]Departamento de Física, Universidade do Minho, Braga;[(f)]Departamento de Física Teórica y del Cosmos, Universidad de Granada, Granada (Spain);[(g)]Dep Física and CEFITEC of Faculdade de Ciências e Tecnologia, Universidade Nova de Lisboa, Caparica;[(h)]Instituto Superior Técnico, Universidade de Lisboa, Lisboa; Portugal.

[140]Institute of Physics of the Czech Academy of Sciences, Prague; Czech Republic.

[141]Czech Technical University in Prague, Prague; Czech Republic.

[142]Charles University, Faculty of Mathematics and Physics, Prague; Czech Republic.

[143]Particle Physics Department, Rutherford Appleton Laboratory, Didcot; United Kingdom.

[144]IRFU, CEA, Université Paris-Saclay, Gif-sur-Yvette; France.

[145]Santa Cruz Institute for Particle Physics, University of California Santa Cruz, Santa Cruz CA; United States of America.

[146][(a)]Departamento de Física, Pontificia Universidad Católica de Chile, Santiago;[(b)]Universidad Andres Bello, Department of Physics, Santiago;[(c)]Instituto de Alta Investigación, Universidad de Tarapacá;[(d)]Departamento de Física, Universidad Técnica Federico Santa María, Valparaíso; Chile.

[147]Universidade Federal de São João del Rei (UFSJ), São João del Rei; Brazil.

[148]Department of Physics, University of Washington, Seattle WA; United States of America.

[149]Department of Physics and Astronomy, University of Sheffield, Sheffield; United Kingdom.

[150]Department of Physics, Shinshu University, Nagano; Japan.

[151]Department Physik, Universität Siegen, Siegen; Germany.

[152]Department of Physics, Simon Fraser University, Burnaby BC; Canada.

[153]SLAC National Accelerator Laboratory, Stanford CA; United States of America.

[154]Physics Department, Royal Institute of Technology, Stockholm; Sweden.

[155]Departments of Physics and Astronomy, Stony Brook University, Stony Brook NY; United States of America.

[156]Department of Physics and Astronomy, University of Sussex, Brighton; United Kingdom.

[157]School of Physics, University of Sydney, Sydney; Australia.

[158]Institute of Physics, Academia Sinica, Taipei; Taiwan.

[159][(a)]E. Andronikashvili Institute of Physics, Iv. Javakhishvili Tbilisi State University, Tbilisi;[(b)]High Energy Physics Institute, Tbilisi State University, Tbilisi; Georgia.

[160]Department of Physics, Technion, Israel Institute of Technology, Haifa; Israel.

[161]Raymond and Beverly Sackler School of Physics and Astronomy, Tel Aviv University, Tel Aviv; Israel.

[162]Department of Physics, Aristotle University of Thessaloniki, Thessaloniki; Greece.

[163]International Center for Elementary Particle Physics and Department of Physics, University of Tokyo, Tokyo; Japan.

[164]Graduate School of Science and Technology, Tokyo Metropolitan University, Tokyo; Japan.

[165]Department of Physics, Tokyo Institute of Technology, Tokyo; Japan.

[166]Tomsk State University, Tomsk; Russia.

[167]Department of Physics, University of Toronto, Toronto ON; Canada.

[168][(a)]TRIUMF, Vancouver BC;[(b)]Department of Physics and Astronomy, York University, Toronto ON; Canada.

[169]Division of Physics and Tomonaga Center for the History of the Universe, Faculty of Pure and Applied

Sciences, University of Tsukuba, Tsukuba; Japan.

[170]Department of Physics and Astronomy, Tufts University, Medford MA; United States of America.

[171]Department of Physics and Astronomy, University of California Irvine, Irvine CA; United States of America.

[172]Department of Physics and Astronomy, University of Uppsala, Uppsala; Sweden.

[173]Department of Physics, University of Illinois, Urbana IL; United States of America.

[174]Instituto de Física Corpuscular (IFIC), Centro Mixto Universidad de Valencia - CSIC, Valencia; Spain.

[175]Department of Physics, University of British Columbia, Vancouver BC; Canada.

[176]Department of Physics and Astronomy, University of Victoria, Victoria BC; Canada.

[177]Fakultät für Physik und Astronomie, Julius-Maximilians-Universität Würzburg, Würzburg; Germany.

[178]Department of Physics, University of Warwick, Coventry; United Kingdom.

[179]Waseda University, Tokyo; Japan.

[180]Department of Particle Physics and Astrophysics, Weizmann Institute of Science, Rehovot; Israel.

[181]Department of Physics, University of Wisconsin, Madison WI; United States of America.

[182]Fakultät für Mathematik und Naturwissenschaften, Fachgruppe Physik, Bergische Universität Wuppertal, Wuppertal; Germany.

[183]Department of Physics, Yale University, New Haven CT; United States of America.

[a] Also at Borough of Manhattan Community College, City University of New York, New York NY; United States of America.

[b] Also at Centro Studi e Ricerche Enrico Fermi; Italy.

[c] Also at CERN, Geneva; Switzerland.

[d] Also at CPPM, Aix-Marseille Université, CNRS/IN2P3, Marseille; France.

[e] Also at Département de Physique Nucléaire et Corpusculaire, Université de Genève, Genève; Switzerland.

[f] Also at Departament de Fisica de la Universitat Autonoma de Barcelona, Barcelona; Spain.

[g] Also at Department of Financial and Management Engineering, University of the Aegean, Chios; Greece.

[h] Also at Department of Physics and Astronomy, Michigan State University, East Lansing MI; United States of America.

[i] Also at Department of Physics and Astronomy, University of Louisville, Louisville, KY; United States of America.

[j] Also at Department of Physics, Ben Gurion University of the Negev, Beer Sheva; Israel.

[k] Also at Department of Physics, California State University, East Bay; United States of America.

[l] Also at Department of Physics, California State University, Fresno; United States of America.

[m] Also at Department of Physics, California State University, Sacramento; United States of America.

[n] Also at Department of Physics, King's College London, London; United Kingdom.

[o] Also at Department of Physics, St. Petersburg State Polytechnical University, St. Petersburg; Russia.

[p] Also at Department of Physics, University of Fribourg, Fribourg; Switzerland.

[q] Also at Dipartimento di Matematica, Informatica e Fisica, Università di Udine, Udine; Italy.

[r] Also at Faculty of Physics, M.V. Lomonosov Moscow State University, Moscow; Russia.

[s] Also at Giresun University, Faculty of Engineering, Giresun; Turkey.

[t] Also at Graduate School of Science, Osaka University, Osaka; Japan.

[u] Also at Hellenic Open University, Patras; Greece.

[v] Also at Institucio Catalana de Recerca i Estudis Avancats, ICREA, Barcelona; Spain.

[w] Also at Institut für Experimentalphysik, Universität Hamburg, Hamburg; Germany.

[x] Also at Institute for Nuclear Research and Nuclear Energy (INRNE) of the Bulgarian Academy of Sciences, Sofia; Bulgaria.

[y] Also at Institute for Particle and Nuclear Physics, Wigner Research Centre for Physics, Budapest;

Hungary.

[z] Also at Institute of Particle Physics (IPP); Canada.

[aa] Also at Institute of Physics, Azerbaijan Academy of Sciences, Baku; Azerbaijan.

[ab] Also at Instituto de Fisica Teorica, IFT-UAM/CSIC, Madrid; Spain.

[ac] Also at Joint Institute for Nuclear Research, Dubna; Russia.

[ad] Also at Moscow Institute of Physics and Technology State University, Dolgoprudny; Russia.

[ae] Also at National Research Nuclear University MEPhI, Moscow; Russia.

[af] Also at Physics Department, An-Najah National University, Nablus; Palestine.

[ag] Also at Physikalisches Institut, Albert-Ludwigs-Universität Freiburg, Freiburg; Germany.

[ah] Also at The City College of New York, New York NY; United States of America.

[ai] Also at TRIUMF, Vancouver BC; Canada.

[aj] Also at Universita di Napoli Parthenope, Napoli; Italy.

[ak] Also at University of Chinese Academy of Sciences (UCAS), Beijing; China.

[*] Deceased